

# The roles of atmospheric wind and entrained water temperature ( $T_e$ ) in the second-year cooling of the 2010–12 La Niña event

Chuan Gao<sup>1,2</sup> · Rong-Hua Zhang<sup>1,3</sup>

Received: 2 September 2015 / Accepted: 20 March 2016 / Published online: 8 April 2016  
© The Author(s) 2016. This article is published with open access at Springerlink.com

**Abstract** An intermediate coupled model (ICM) yields a successful real-time prediction of the sea surface temperature (SST) evolution in the tropical Pacific during the 2010–12 La Niña event, whereas many other coupled models fail. It was previously identified that the thermocline effect on the SST (including vertical advection and mixing), as represented by water temperature entrained into the mixed layer ( $T_e$ ) and its relationship with the thermocline fluctuation, is an important factor that affects the second-year cooling in mid-late 2011. Because atmospheric wind forcing is also important to ENSO processes, its role is investigated in this study within the context of real-time prediction of the 2010–12 La Niña event using the ICM in which wind stress anomalies are calculated using an empirical model as a response to SST anomalies. An easterly wind anomaly is observed to persist over the western-central Pacific during 2010–11, which acts to sustain a horse shoe-like  $T_e$  pattern connecting large negative subsurface thermal anomalies in the central-eastern regions off and on the equator. Sensitivity experiments are conducted using the ICM to demonstrate how its SST predictions are directly affected by the intensity of wind forcing. The second-year cooling in 2011 is not predicted to occur in the ICM if the easterly wind anomaly intensity is weakly

represented below certain levels; instead, a surface warming can emerge in 2011, with weak SST variability. The results of the current study indicate that the intensity of interannual wind forcing is equally important to SST evolution during 2010–11 compared with that of the thermocline effect. To correctly predict the observed La Niña conditions in the fall of 2011, the ICM needs to adequately represent the intensity of both the wind forcing and the thermocline effects.

**Keywords** The 2010–2012 La Niña event · Wind forcing · Thermocline effect · Coupled model

## 1 Introduction

The El Niño-Southern Oscillation (ENSO) is a natural climate phenomenon centered in the tropical Pacific, which influences climate variability and predictability worldwide. In the past three decades, extensive ENSO studies have made remarkable progress (e.g., see the TOGA special issue of JGR-Oceans, 1998; McPhaden et al. 2006). For example, various feedback processes have been identified that can be responsible for ENSO cycles in the tropical Pacific. As understood, ENSO originates from air-sea interactions in the tropical Pacific (Bjerknes 1969), involving a positive feedback loop among the SST, wind and the thermocline in the tropical Pacific (the so-called thermocline feedback; e.g., Jin and An 1999). The loop of the positive thermocline feedback includes two elements, one related to the anomalous temperature of water entrained into the mixed layer ( $T_e$ ), which affects the SST and is affected by the thermocline (referred as the thermocline effect); another element is associated with wind forcing, which affects the ocean and is affected by the SST. In addition, to interpret

✉ Rong-Hua Zhang  
rzhang@qdio.ac.cn

<sup>1</sup> Key Laboratory of Ocean Circulation and Waves,  
Institute of Oceanology, Chinese Academy of Sciences,  
Qingdao 266071, China

<sup>2</sup> University of Chinese Academy of Sciences, Beijing 100029,  
China

<sup>3</sup> Function Laboratory for Ocean and Climate Dynamics,  
Qingdao National Laboratory for Marine Science  
and Technology, Qingdao 266237, China

the ENSO's cyclic nature, negative feedback processes have also been proposed. They include a delayed oscillator paradigm associated with the effects of wave reflections from the western boundaries of the tropical Pacific (Schopf and Suarez 1988; Battisti and Hirst 1989), the charge/discharge processes due to Sverdrup transport (Jin 1997), the western Pacific wind-forced Kelvin wave effects (Weisberg and Wang 1997; Wang et al. 1999), and the anomalous zonal advection processes (Picaut et al. 1997). As shown in the unified oscillator (Wang 2001; Wang and Picaut 2004), these negative feedbacks may work together for terminating El Niño, with their relative importance varying with time. Additionally, local processes in the central-eastern equatorial Pacific are important to SST variability, including thermal influences from off-equatorial regions (Gu and Philander 1997; Zhang et al. 2008).

Furthermore, after Cane et al. (1986) and Zebiak and Cane (1987), various coupled ocean–atmosphere models have been developed to improve real-time ENSO predictions (e.g., Barnett et al. 1993; Chen et al. 1995; Ji et al. 1996; Latif et al. 1998; Kirtman et al. 2002; Zhang et al. 2003; Luo et al. 2005; Saha et al. 2006; Zheng et al. 2006; Wang et al. 2010; Stockdale et al. 2011; Zhu et al. 2012, 2014). In particular, reasonable predictions can now be made 6 months and longer in advance (e.g., Barnston et al. 2012; see the summary of model ENSO forecasts at the International Research Institute for Climate and Society (IRI) website: <http://iri.columbia.edu/climate/ENSO/currentinfo/update.html>). Presently, more than 20 models with different degrees of complexity have been routinely used to make real-time forecasts of the SST in the equatorial Pacific (Barnston et al. 2012; see the details at the IRI website).

During 2010–12, the tropical Pacific experienced a prolonged La Niña condition, with a second-year sea surface cooling event that occurred in the fall of 2011 (e.g., Hu et al. 2014; Zhang et al. 2013; Feng et al. 2015). However, many coupled models fail to forecast the Niño 3.4 SST cooling when initialized from early-mid 2011 (see the details at the IRI website). Very few coupled models make a good prediction of the 2010–11 cold SST conditions in the tropical Pacific; see the IRI web site and the summary online at [http://www.nws.noaa.gov/ost/climate/STIP/r+d/board\\_op4.html](http://www.nws.noaa.gov/ost/climate/STIP/r+d/board_op4.html). This difficulty represents a great challenge to the ENSO research and prediction communities, indicating a clear need to understand why so many coupled models fail to forecast the second-year cooling at a lead time of 6 months or so and to find a way to effectively improve real-time ENSO predictions. This double-dip cooling event during 2010–12 provides an opportunity to address these important related issues.

Various factors are involved in the second-year cooling phenomenon in 2011 (e.g., Hu et al. 2014; Zhang et al. 2013), including processes in the atmosphere and ocean, at

the sea surface and subsurface depths, and on and off the equator. As the thermocline feedback involves interactions among the SST, wind and the thermocline, the intensities of wind forcing and thermocline effect (as indicated in  $T_e$ ) are both important to SST variability in the tropical Pacific. On interannual time scales,  $T_e$  is a primary factor affecting SST evolution in the equatorial Pacific; surface wind is a major forcing factor to the thermocline in the equatorial Pacific, thus being an important source for  $T_e$  variability. So, these two elements (wind and  $T_e$ ) are closely related with each other in terms of their effects on SST evolution as represented in the positive thermocline feedback loop.

We developed an intermediate coupled model (ICM) for ENSO-related modeling, with a focus on the role of the thermocline effect (Zhang et al. 2003, 2005a, b). The ICM is an anomaly model consisting of an intermediate ocean model (IOM) and an empirical wind stress model. One crucial component of the ICM is the way in which the subsurface entrainment temperature in the surface mixed layer ( $T_e$ ) is explicitly parameterized in terms of the thermocline variability [as represented by sea level (SL)]. An optimized procedure is developed to depict  $T_e$  using inverse modeling from an SST anomaly equation and its empirical relationship with SL variability (Zhang et al. 2005a). Additionally, interannual anomalies of wind stress ( $\tau$ ) are represented as a response to those of SST. Correspondingly, interannual anomalies of  $T_e$  and  $\tau$  are determined by their statistical models, written respectively as  $T_e = \alpha_{T_e} \cdot F_1(\text{SL})$  and  $\tau_{\text{inter}} = \alpha_{\tau} \cdot F_2(\text{SST})$ , in which  $F_1$  and  $F_2$  are the relationships between  $T_e$  and SL and between  $\tau$  and SST derived using statistical methods from historical data;  $\alpha_{\tau}$  and  $\alpha_{T_e}$  are two parameters introduced to represent their intensities (they are tunable and can be prescribed as a constant in coupled simulations). Note that this ICM has been routinely used for real-time ENSO prediction since 2003 (see details at <http://iri.columbia.edu/climate/ENSO/currentinfo/update.html>). In particular, this model is one of the coupled models that make a good prediction of cold SST conditions in the tropical Pacific during 2010–12 (Zhang et al. 2013). Thus, the ICM offers an opportunity to reveal the roles of the wind forcing and thermocline effect in the second-year cooling in 2011 by proper tuning of  $\alpha_{\tau}$  and  $\alpha_{T_e}$ .

In a previous study (Zhang et al. 2013), we used the ICM to demonstrate the role played by the thermocline effect in the second-year cooling in 2011. We find that the explicit  $T_e$  parameterization based on the relation with sea level (SL) in the ICM enhances the ability to forecast the 2010–11 La Niña events. In particular, it is shown that the magnitude of negative  $T_e$  anomalies persisting in the central-eastern equatorial Pacific is an important factor affecting the second-year cooling in 2011. Another noticeable feature associated with the SST evolution during 2010–12 is the persistence of easterly wind anomalies in the western-central

equatorial Pacific. As indicated within the positive thermocline feedback loop, the intensity of interannual wind forcing is also important to ENSO processes.

In this study, we investigate the role played by wind forcing in the second-year cooling in 2011 using the ICM (Zhang et al. 2003, 2005a, b, 2013). The intensity of wind forcing in the ICM can be conveniently changed by tuning  $\alpha_\tau$  so that its effects on SST predictions can be quantified for the 2010–12 years. Furthermore, as the wind stress and  $T_e$  are participating in the same thermocline feedback loop, they can have similar modulating effects on the SST cooling in 2011, but they have not been revealed in a coherent way. By comparing the role of atmospheric wind forcing with that of subsurface thermal forcing in the SST evolution during 2010–12, the relative effects of the two elements can be illustrated from a prediction point of view. It will be seen below that subsurface thermal effect and surface wind forcing act to play an equivalent role in the second-year cooling in 2011.

This paper is organized as follows. Section 2 describes the model and its prediction procedures. Section 3 provides a brief description of the evolution observed in 2010–12, followed by the ICM-based simulation and prediction in Sect. 4. Section 5 addresses the role of wind forcing in the second-year cooling in 2011, followed by a comparative analysis for the role of the thermocline effect in Sect. 6. A discussion and conclusion are given in Sect. 7.

## 2 The ICM and its real-time prediction procedures

The roles of the thermocline and wind forcing effects in the second-year cooling in 2011 are examined using an intermediate coupled model (ICM) consisting of an intermediate ocean model (IOM) and a statistical wind stress model of the tropical Pacific. The details can be found in Zhang et al. (2003, 2005a, b). Its dynamic ocean component is an intermediate complexity model developed by Keenlyside and Kleeman (2002) that was based on the previous baroclinic modal decomposition method in the vertical (McCreary 1981). Different from the commonly used Zebiak–Cane model (1987), this relatively newly developed ICM takes into account the spatially varying stratification and the realistic vertical structure of the upper ocean (e.g., ten vertical modes are included). In addition, nonlinear effects are partially considered in the momentum equation determining the zonal and meridional currents. As a result, this dynamic ocean model yields realistic simulations of mean equatorial circulation and its variability in the tropical Pacific.

An SST anomaly model is incorporated into this ocean dynamical model to represent thermodynamic processes of the surface mixed layer. Another distinguished feature

added to this ocean model is an empirical parameterization for the temperature of subsurface water entrained into the mixed layer ( $T_e$ ), written as  $T_e = \alpha_{T_e} \cdot F_1(SL)$ , in which SL is sea level anomalies;  $F_1$  represents the relationships between interannual variations in  $T_e$  and SL which is determined using an EOF technique from historical data (Zhang et al. 2005b);  $\alpha_{T_e}$  is a scalar parameter introduced to represent the  $T_e$  effect intensity. In practice,  $T_e$  can be derived in a way that subsurface thermal effects on SST are optimized with a given SST anomaly equation (Zhang et al. 2005a). A novel approach is developed to optimize  $T_e$  by performing inverse modeling of an SST anomaly equation. As demonstrated by Zhang et al. (2005a), the ocean model can realistically simulate interannual SST variability in the tropical equatorial Pacific because the improved  $T_e$  calculation adequately represents the subsurface effect on SST variability due to the vertical processes in the equatorial Pacific.

Furthermore, an ICM is formed for the tropical Pacific by coupling the ocean model to a simple statistical model for interannual wind stress anomalies ( $\tau_{inter}$ ), written as  $\tau_{inter} = \alpha_\tau \cdot F_2(SST)$ , in which  $F_2$  is the relationships derived using a singular value decomposition (SVD) method from historical data, and  $\alpha_\tau$  is a parameter introduced to represent the intensity of wind response to SST anomalies.

Interannual anomalies in the tropical Pacific are produced by the ICM with its components exchanging the anomaly fields within the coupled system (Fig. 1). At each time step, the dynamical ocean model calculates anomaly fields of oceanic currents and pressure fields, including SL anomalies, anomalous currents over the surface mixed layer and vertical velocity at the base of the mixed layer. Then, SST anomalies are calculated using its anomaly equation. Using the  $\tau$  model, the produced SST anomaly is used to calculate wind stress anomalies, which are used to force the ocean dynamical model. Information is exchanged once daily between the atmosphere ( $\tau$ ) and the ocean (SST), and the  $T_e$  anomaly and SL anomaly. The ICM is initiated with an imposed westerly wind anomaly for eight months. The evolution of anomalous conditions thereafter is determined solely by the coupled ocean–atmosphere interactions in the system.

In this coupled system, the two dominant forcing fields ( $\tau$  for the ocean and  $T_e$  for the SST) are both determined using statistical methods. Two scalar parameters are introduced to represent the intensity of wind forcing and thermocline effect ( $\alpha_\tau$  and  $\alpha_{T_e}$ ). Experiments indicate that the ICM with  $\alpha_\tau = 1.0$  and  $\alpha_{T_e} = 1.0$  can well depict ENSO cycles having an approximately 4-year oscillation period; this case is referred to as a standard run (Zhang et al. 2005b). The ICM with varying values of  $\alpha_\tau$  and  $\alpha_{T_e}$  gives rise to a weakened or amplified interannual variability with oscillation periods of 4 years nearly unchanged. In addition, Zhang and Gao (2015) illustrated a new mechanism for the onset of El Niño events as appeared in the ICM.

## Prediction Initialization

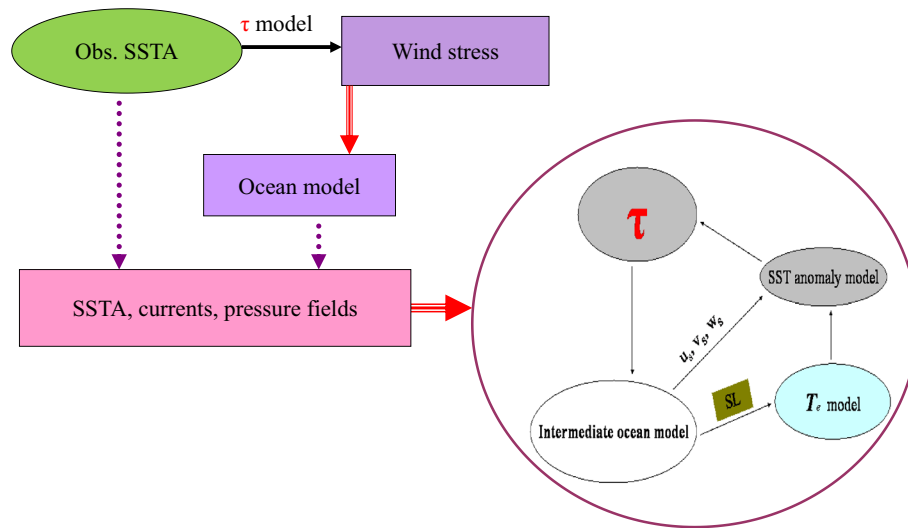


**Fig. 1** A schematic diagram showing the real-time prediction procedure to initialize the ICM consisting of an ocean dynamical model, an SST anomaly model, an empirical model to calculate interannual  $T_e$  anomalies from SL, and a statistical atmospheric model to calculate interannual wind stress anomalies ( $\tau_{\text{inter}}$ ) from SST. Here, observed interannual SST anomalies are the only field which is considered in the coupled prediction. Taking a prediction made on 1 January 2011 as an example, a temporal succession of daily SST fields is formed

As the ICM can realistically depict the spatial structure and time evolution of interannual SST variability, it provides the basis for real-time SST predictions in the tropical Pacific. Real-time predictions using the ICM are made as follows (Fig. 1). A simple procedure is taken in which the observed interannual SST anomalies are the only field used in the prediction initialization (Zhang et al. 2013). In real-time prediction practice, experiments are usually conducted around the middle of each month, when monthly mean SST fields from the previous month and weekly mean SST fields from the first week of the current month are available from NOAA's Environment Modeling Center (EMC; Reynolds et al. 2002), which can be obtained online at the IRI data library. Taking a prediction made on 1 January 2011 as an example, a linear interpolation method is adopted to form a temporal succession of daily SST fields from the observed monthly SST data historically from 1980 through December 2010 and from the weekly SST data in early January 2011; then, the  $\tau_{\text{inter}}$  field is derived using its empirical model as a response to the observed SST anomalies. The derived  $\tau_{\text{inter}}$  fields historically up to early January 2011 are taken to force the ocean model to produce an initial ocean state for the first day of each month (i.e., 1 January 2011), from which predictions are made using the ICM. Note that the ICM is an anomaly model in which interannual

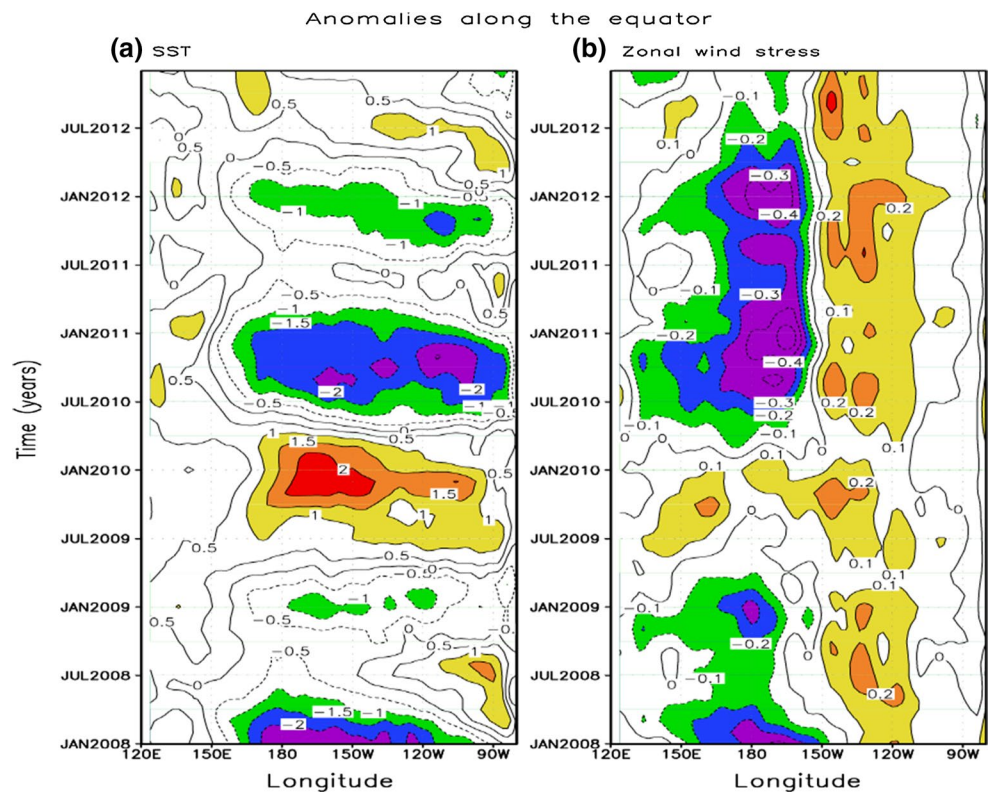
using a linear interpolation from observed monthly SST data historically from 1980 through December 2010 and from weekly SST data in early January 2011. The  $\tau_{\text{inter}}$  field is then derived using its empirical model from the SST anomalies. The derived  $\tau_{\text{inter}}$  field historically up to early January 2011 is used to force the ocean model to generate an initial ocean state for 1 January 2011, from which a prediction is made forward using the ICM

SST anomalies are directly produced; there is no correction or adjustment made to the ICM-produced SST anomaly fields. Since 2003, this ICM has been routinely used to predict SST conditions in the tropical Pacific for lead times out to 12 months; real-time forecasts are routinely released online at the IRI ENSO web site. As the amplitude of the calculated  $T_e$  and  $\tau$  anomalies (tunable by using  $\alpha_\tau$  and  $\alpha_{T_e}$ ) is important to ENSO evolution, sensitivity experiments with different values of  $\alpha_\tau$  and  $\alpha_{T_e}$  are conducted to examine the effects of wind and thermocline forcings on the second-year cooling in 2011.

### 3 Observed evolution during 2010–12

Various observed and reanalysis data are used to validate model simulations and predictions, including SST fields from Reynolds and Smith (1994) and wind stress from the NCEP/NCAR reanalysis (Kalnay et al. 1996). Oceanic temperature and salinity data are from the gridded Argo products provided by the International Pacific Research Center (IPRC)/Asia–Pacific Data-Research Center (APDRC), which include monthly and long-term climatological mean fields spatially averaged onto  $1^\circ$  grids. Monthly mixed layer depth (MLD) and  $T_e$  data are also available directly from the

**Fig. 2** Zonal-time sections along the equator for **a** observed SST anomalies and **b** the NCEP/NCAR reanalysis zonal wind stress. The contour interval is  $0.5\text{ }^{\circ}\text{C}$  for SST and is  $0.1\text{ dyn cm}^{-2}$  for zonal wind stress



IPRC/APDRC Argo products. Gridded sea level anomalies are from the Ssalto/Duacs multimission altimeter products distributed by *Aviso* with support from Cnes, which are available online at <http://www.aviso.oceanobs.com/duacs/>.

Figures 2 and 3 display examples for observed SST anomalies and reanalyzed wind stress anomalies from the NCEP/NCAR. A moderate to strong La Niña episode prevailed in 2010 (also see the Tropical Atmosphere Ocean (TAO) real-time data online at <http://www.pmel.noaa.gov/tao/>). During April–July 2011, neutral SST conditions appeared in the eastern equatorial Pacific and the La Niña seemed to be ending in the spring of 2011. However, weak La Niña conditions re-emerged in early August 2011 and grew to weak/moderate strength during November 2011. A striking feature observed here was the appearance of the second-year surface cooling in the boreal fall of 2011. In the atmosphere, pronounced easterly wind anomalies were observed to persist over the central equatorial basin in 2010–12 (Figs. 2b, 3). As such, the La Niña conditions were observed to sustain in the central-eastern equatorial Pacific during 2011–12.

In the subsurface ocean, La Niña-induced thermal anomalies prevailed in the equatorial Pacific during 2010–12. For example, Zhang et al. (2013) examined the structure of subsurface thermal conditions (as represented in  $T_e$ ), which was characterized by a horseshoe-like  $T_e$  pattern during 2010–12. In the central-eastern equatorial Pacific, negative  $T_e$  anomalies prevailed during 2010–11.

In the western tropical region, positive subsurface thermal anomalies accumulated during 2010 and early 2011. The positive heat content anomalies in the west were observed to extend eastward along the equator in early 2011, acting to weaken the cold SST anomalies in the east during the spring of 2011, with a tendency to reverse the La Niña conditions. Indeed, a nearly neutral SST condition emerged in the eastern equatorial Pacific in mid 2011. However, during this period, large negative  $T_e$  anomalies persisted in the central-eastern equatorial basin, which acted to prevent the eastern equatorial Pacific from transitioning into a warm SST state that can be attributed to the eastward propagation of the positive heat content anomalies from the western regions. In addition, the large persistent negative subsurface thermal anomalies on the equator were seen to have their connections to subsurface thermal variability off the equator. Thus, the persistent negative  $T_e$  anomalies in the central equatorial Pacific play an important role in sustaining SST cooling during summer–fall 2011 (Fig. 3d, e). The related cold SST anomalies were accompanied by easterly wind anomalies (Fig. 3d, e). These SST and wind anomalies were seen to amplify through ocean–atmosphere coupling, leading to the second-year cooling. As a result, a weak La Niña condition re-emerged over the tropical Pacific in the fall of 2011. These features can be clearly seen from the tropical atmosphere–ocean (TAO) observations online at <http://www.pmel.noaa.gov/tao/>.

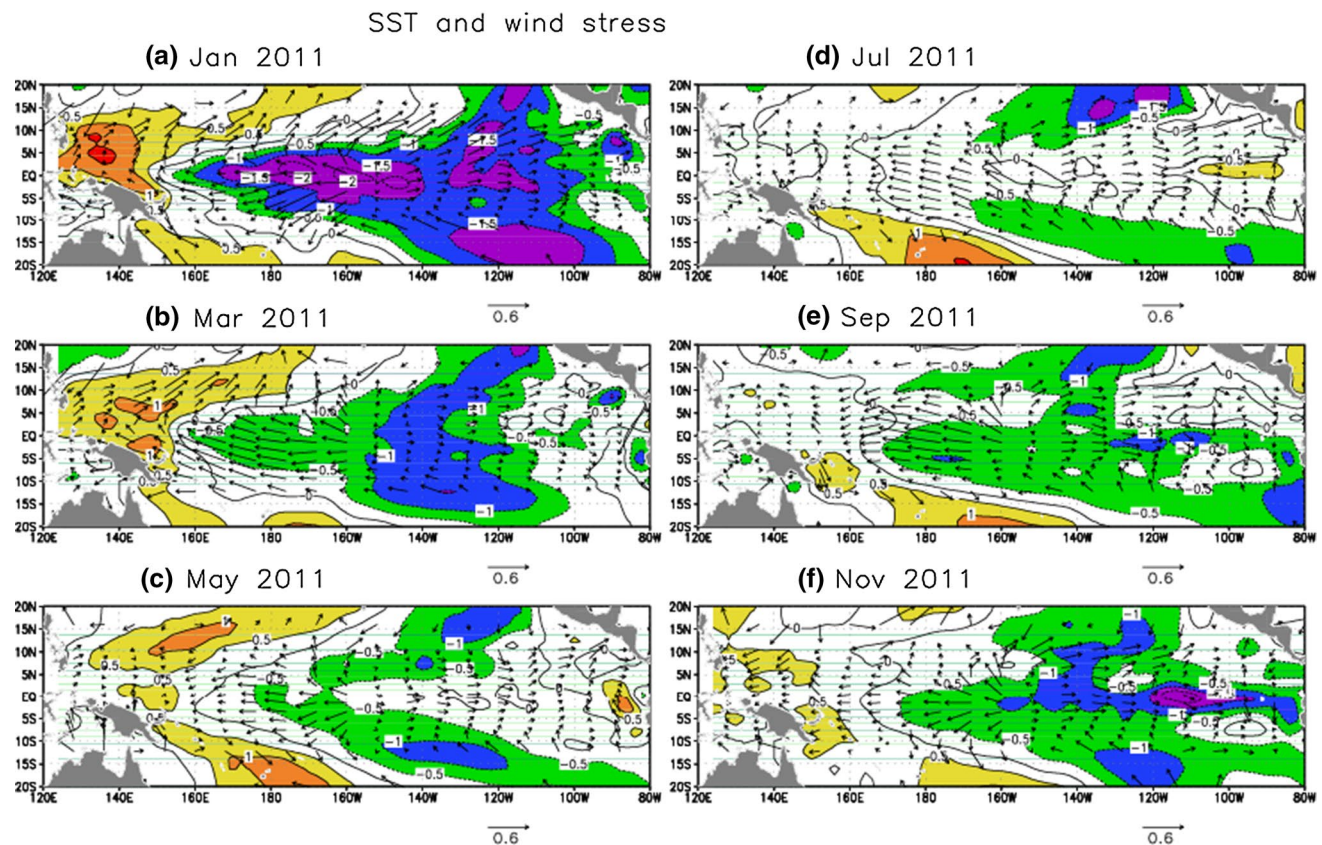


**Fig. 3** Horizontal distributions of observed SST anomalies (contours) and the NCEP/NCAR reanalysis wind stress anomalies (vectors) for **a** Jan. 2011, **b** Mar. 2011, **c** May 2011, **d** Jul. 2011, **e** Sep.

2011 and **f** Nov. 2011. The contour interval is  $0.5\text{ }^{\circ}\text{C}$  for SST and is  $\text{dyn cm}^{-2}$  for wind stress

## 4 The ICM-based simulation and prediction

As part of an initialization procedure, observed SST anomalies are taken to derive wind stress anomalies, which in turn are used to force the ocean component of the ICM to obtain ocean state from which predictions are made. In this section, outputs from the ocean-only simulations forced by the derived wind anomalies are analyzed to describe processes affecting the second-year cooling of the 2010–12 La Niña condition. Then, the ICM is used to make real-time predictions to illustrate its performance. These results are presented below.

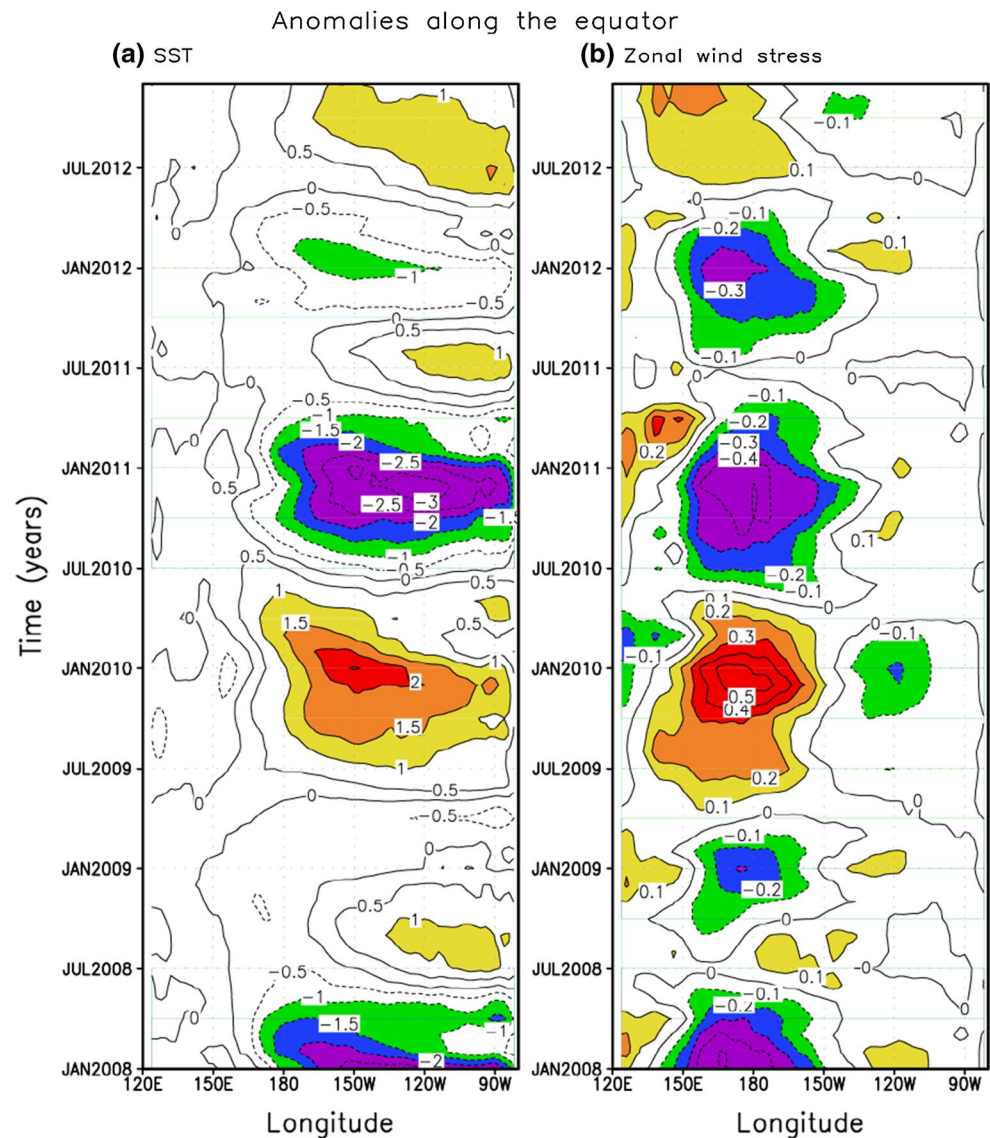
### 4.1 Processes affecting the second-year cooling in 2010: The forced ocean experiments

Interannual anomalies of wind stress derived from the  $\tau_{\text{inter}}$  model and those of SST, SL and  $T_e$  simulated from the ocean-only experiment are shown in Figs. 4, 5. It is seen that the ocean component of the ICM can well simulate these interannual anomalies. As observed, the model captures well the La Niña conditions in 2010–12 (Fig. 4a). For

example, after the La Niña in 2010, negative SST anomalies in the east began to weaken from early 2011, and the La Niña conditions decayed gradually and transitioned to a slightly above-normal SST condition in mid 2011. Then, cold conditions reappeared in mid 2011 through ocean–atmosphere coupling, leading to the second-year cooling in the fall of 2011.

Further, coherent relationships among these anomalies (SL,  $T_e$ , SST and winds) produced in the model can be used to illustrate processes leading to the surface cooling in the summer and fall of 2011. For example, starting from late 2010, when the La Niña condition prevailed in the eastern basin, the development into the second-year cooling in 2011 involved multiple processes. On the oceanic side, SL anomalies (an indicator of the thermocline variability) were positive in the west during 2010 and were seen to extend eastward along the equator (Fig. 5b), exerting an influence on  $T_e$  and SST in the east during 2011 (Zhang et al. 2013). The arrival of the positive SL anomaly to the east in April–June 2011 acted to weaken cold SST anomalies in the east (Fig. 4a). Regionally in the central-eastern equatorial Pacific, however, a pronounced negative  $T_e$  anomaly

**Fig. 4** Zonal-time sections of anomaly fields along the equator simulated from the ICM for **a** SST and **b** zonal wind stress. The contour interval is  $0.5\text{ }^{\circ}\text{C}$  for SST and  $0.1\text{ dyn cm}^{-2}$  for zonal wind stress



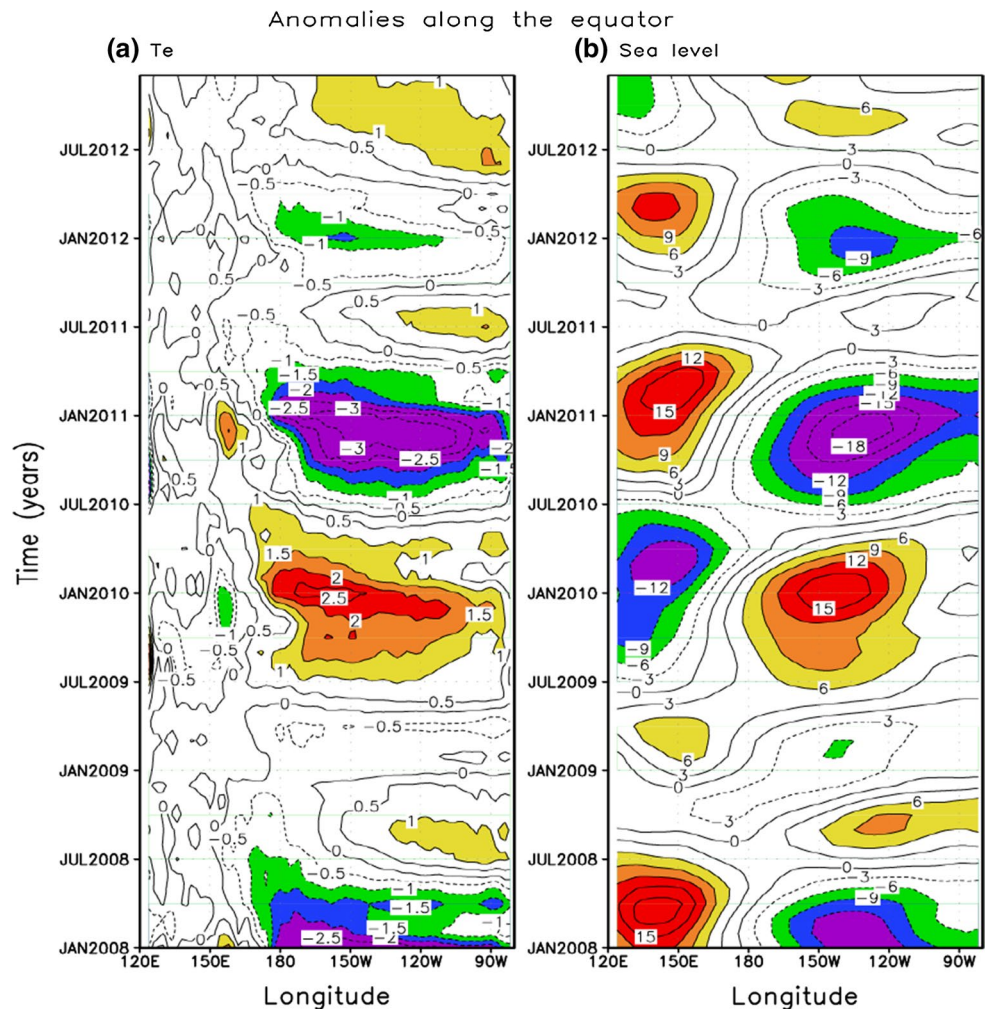
persisted in 2010–2011 (Fig. 5), tending to maintain a cold SST condition in the east. On the atmospheric side, easterly wind anomalies persisted over the western and central Pacific (Fig. 4b), acting to elevate the thermocline and to sustain the negative  $T_e$  anomalies in the central-eastern equatorial Pacific.

To illustrate the space–time evolution in more details, Fig. 6 shows snapshots of related anomaly fields at different periods during the second-year cooling event. These maps start with the La Niña conditions in Jan. 2011, proceeded to a near-neutral condition in June 2011 (as indicated by the SST signal), and continued to a second-year cooling condition in Oct. 2011. Together with Figs. 4 and 5, the spatial structure and phase relationships among anomalies of SL,  $T_e$ , SST and surface winds can be more clearly illustrated off and on the equator during the evolving periods.

For instance, during the La Niña event in 2010, there was a buildup of warm waters in the western Pacific Ocean due to stronger-than-normal trade winds in the central basin, with the SL in the west increasing steadily. The subsequent evolution into the second-year cooling in 2011 was affected by several factors. Looking at subsurface anomalies (as represented by SL), propagating SL signals were evident around the basin (Figs. 5b, 6), remotely influencing  $T_e$  and SST (Figs. 4a, 5a). Off the equator, for example, large negative SL anomalies in the east, produced by La Niña condition in 2010, propagated westward in the tropical North Pacific. This off-equatorial negative SL anomaly was seen to extend onto the equator near the date line in 2011, sustaining the negative  $T_e$  anomalies (Fig. 6).

On the equator, a positive SL anomaly propagated eastward in early 2011 (Figs. 5b, 6). Its arrival to the east in the middle of 2011 induced a warm SST condition in the

**Fig. 5** Zonal-time sections of anomaly fields along the equator simulated from the ICM for **a**  $T_e$  and **b** SL. The contour interval is  $0.5\text{ }^{\circ}\text{C}$  for  $T_e$  and  $3\text{ cm}$  for SL



east, but the effect on the SST was not to be sufficiently strong to sustain it. The persistent negative  $T_e$  anomalies in the central-eastern regions acted to sustain the cold SST anomalies, which were accompanied by easterly wind anomalies in the west. The related anomalies of SST and surface winds were seen to amplify through their coupling (Fig. 4). A systematic cold SST anomaly was seen in the east in August 2011. By the fall of 2011, there were noticeable signs of the development of cold conditions at the sea surface. The second-year cooling reemerged in the tropical Pacific in late 2011.

Based on these analyses, a schematic diagram is given in Fig. 7 showing factors responsible for the second-year SST cooling in the equatorial Pacific. Several processes tended to affect SST conditions in 2011. In the atmosphere, easterly wind anomalies were present near and west of the date line during 2010–11. These anomalies acted to elevate the thermocline, giving rise to negative  $T_e$  anomalies in the central-eastern equatorial Pacific. One pronounced feature in  $T_e$  was a horse shoe-like pattern in the equatorial Pacific during 2010–11, with its negative anomaly center

located in the central equatorial Pacific. Following the La Niña event in 2010 (Fig. 3a), there was a downwelling signal off the equator in the western Pacific that propagated westward to the western boundary in late 2010 (as Rossby waves; Fig. 6). In early 2011, large positive SL anomalies were present in the western boundary regions (Fig. 6b), where a positive SL anomaly originated as a reflected signal (Fig. 5b) and propagated eastward on the equator during early 2011 (as equatorial Kelvin waves; Fig. 5b). Its arrival to the east in middle 2011 acted to weaken the cold SST anomalies there. Indeed, there appeared a nearly neutral SST condition in the east in mid 2011 (Fig. 4a). However, large negative  $T_e$  anomalies still persisted in the central-eastern equatorial Pacific during 2010–11, tending to sustain cold SST condition in the east. Additionally, during and after the La Niña event in 2010, negative SL anomalies propagated westward off the equator; their extension into the central equatorial region acted to reinforce the negative  $T_e$  anomalies in the central basin. Additionally, the negative subsurface thermal anomalies off the equator penetrated into the central-eastern equatorial Pacific, further fostering



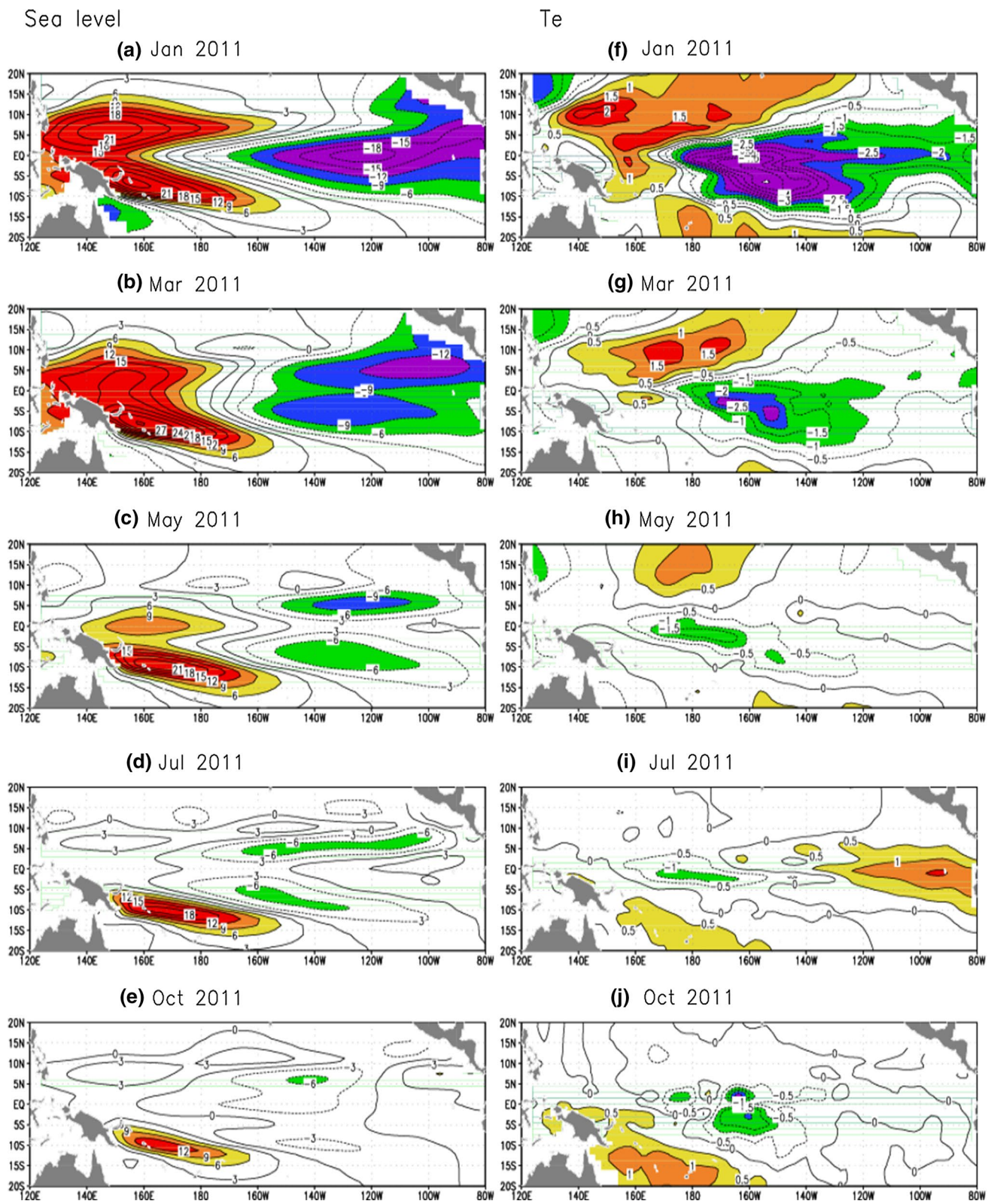


**Fig. 6** Horizontal distributions of SL (the left panels) and  $T_e$  (the right panels) anomalies simulated using the ocean component of the ICM for a, f Jan. 2011, b, g Mar. 2011, c, h May 2011, d, i Jul. 2011 and e, j Oct. 2011. The contour interval is 3 cm for SL and 0.5 °C for  $T_e$ .

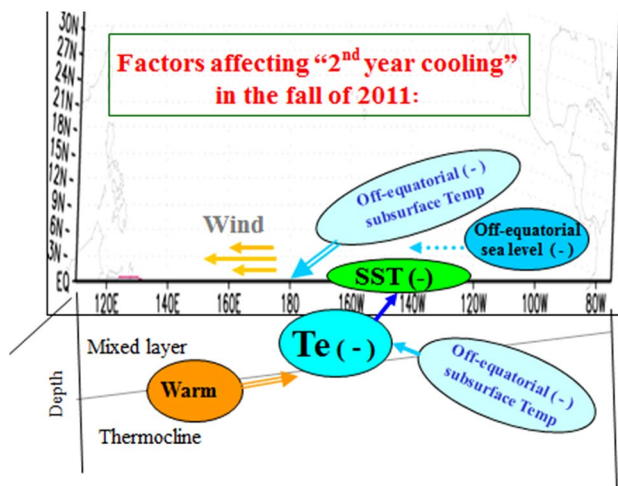


**Fig. 7** A schematic diagram showing processes affecting cold SST conditions in the central-eastern equatorial Pacific during 2011. In the central equatorial Pacific, large negative  $T_e$  anomalies were seen to persist throughout 2010–11, with a horse shoe-like pattern connecting subsurface thermal variability off and on the equator. A few processes tended to sustain this  $T_e$  pattern. On the atmospheric side, easterly wind anomalies were present near and west of the date line during 2010–11, which acted to elevate the thermocline, giving rise to negative  $T_e$  anomalies in the central domain. On the oceanic side, negative subsurface thermal anomalies off the equator were seen to emerge onto the equator in the central basin, fostering the negative  $T_e$  anomalies on the equator. Additionally, during and after the La Niña event in 2010, negative SL anomalies were seen to propagate westward off the equator from the eastern boundary regions; their extension into the central equatorial Pacific acted to reinforce the negative  $T_e$  anomalies in the central basin. In the western equatorial Pacific, a positive subsurface thermal anomaly persisted during 2010–11 and was seen to propagate eastward along the equator in spring 2011; its arrival to the east in mid-2011 acted to weaken the cold conditions in the eastern equatorial Pacific. Thus, the fate of SST condition in the east is determined by the two counteracting effects: warming from the western Pacific and cooling locally associated with the negative  $T_e$  anomalies in the central-eastern equatorial Pacific

the negative  $T_e$  anomalies on the equator. Thus, several processes collectively acted to sustain the negative  $T_e$  anomalies in the central equatorial region during 2010, which were essential for the reappearance of the cold SST condition in July–August 2011.

Evidently, two competing processes were at work in determining the SST condition in the eastern equatorial Pacific in 2011: a warming effect from the western tropical Pacific and a cooling effect locally associated with the negative  $T_e$  anomalies. The latter was further associated with easterly wind forcing. The fate of the SST condition was thus determined by the effect which is dominant. Since SSTs became cold in 2011, the warming effect from the west was not strong enough to reverse the cooling condition associated with the 2010 La Niña event in the east, but the negative  $T_e$  anomaly effect appeared to play a dominant role in

sustaining the cold SST condition in 2011. In mid and late 2011, a SST cooling re-emerged in the east, accompanied by easterly wind anomalies over the western regions (Fig. 4).

Note that there were westerly wind anomalies in the far western Pacific during the spring of 2011 (Fig. 3a, b), which can force oceanic Kelvin waves. As such, the warming effect coming from the westerly wind-forced Kelvin waves from the west can potentially change the sign of the SST anomaly in the central and eastern Pacific (Weisberg and Wang 1997; Wang et al. 1999). However, the amplitude of the westerly wind anomalies on the equator in the western Pacific was small and the corresponding westerly wind-forced Kelvin waves were not strong enough to terminate the cooling conditions in the central and eastern Pacific, and thus the second-year cooling sustained in 2011.

Numerous previous studies also examined the prolonged La Niña events, which was frequently occurred in the past (Okumura and Deser 2010; Hu et al. 2014; Lee et al. 2014; DiNezio and Deser 2014). For example, Lee et al. (2014) summarized that ENSO events can be categorized as the transition and resurgence ones and the second-year cooling in 2011 was considered as the resurgence of the 2010 La Niña. DiNezio and Deser (2014) argued that the thermocline effect was key for the return of La Niña, and that the 2010–12 La Niña event belonged to a continued La Niña case. Our results are consistent with these previous studies.

#### 4.2 Prediction using the ICM

Figure 8 presents examples for the predicted Niño 3.4 SST anomalies during 2011–12 from various coupled models (Barnston et al. 2012). Observations indicated a prolonged La Niña condition in the tropical Pacific during the period 2010–12, with the second-year cooling in mid-late 2011 that followed a major peak cooling in October 2010. The real-time SST predictions exhibited a large spread among different models. Strikingly, many models failed to depict the second-year cooling in the fall of 2011 when forecasted from initial conditions on 1 June 2011.

As previously examined (Zhang et al. 2013), the so-called ESSIC ICM (the ICM used at the Earth System Science Interdisciplinary Center (ESSIC), University of Maryland; Barnston et al. 2012) can realistically forecast the SST evolution observed during 2010–11. For example, the predicted SST anomalies from the ICM followed the corresponding observations very closely (Fig. 8). The observed SST evolution exhibited two turning points, one in June 2011 from warming to cooling, and the other in January 2012 from cooling to warming. In early 2011, the La Niña condition was decaying, and SSTs became near normal in mid-July; a return of La Niña conditions was seen in the

fall of 2011, and these conditions persisted into early 2012, when SST evolution underwent another transition to warming in the tropical Pacific.

Figures 9, 10, 11 and 12 present the detailed space–time distributions of various anomalies predicted from the ICM with  $\alpha_\tau = 1.0$  and  $\alpha_{T_e} = 1.0$ ; the corresponding observations can be seen in Figs. 2 and 3 and can also be found at the CPC's monthly ocean briefing web site which provides real-time diagnostic and prediction discussions. As analyzed from observations and the ocean-only forced simulation above, the ICM can realistically predict the onset and development of the second-year cooling even from initial conditions on 1 January 2011. For instance, the appearance of the cold SST anomalies in 2011 was captured well by the ICM. As examined above, the cold SST anomalies in the central-eastern region were affected by several processes in the ocean, which were represented well in the ICM-based prediction. For example, during the year 2010 when a La Niña condition was underway in the tropical Pacific, positive heat content anomalies, which were accumulated in the western Pacific, tended to propagate eastward along the equator in early 2011, acting to have a remote warming effect on SST in the east. At the same time, negative subsurface anomalies (as indicated by  $T_e$ ) persisted locally over the central-eastern equatorial Pacific, with their connection to thermal anomalies off the equator. Additionally, an easterly wind anomaly was seen to persist in the

western-central equatorial Pacific, which acted to maintain the negative  $T_e$  anomaly pattern.

The coupled ocean–atmosphere system in the tropical Pacific can evolve into a warming or a cooling condition in year 2011, depending on the relative dominance of these two competing processes: the warming effect remotely from the west (that was associated with the positive heat content anomalies which were produced during the La Niña in 2010) and the cooling effect locally associated with the large negative  $T_e$  anomalies (that persisted over the central-eastern equatorial Pacific). If the former dominated the latter, a warm condition could develop in the fall of 2011; otherwise, a cold condition can persist and prevailed. The fact that the SSTs in the east became cooling in mid-late 2011 indicated that the latter (the cooling effect locally associated with the persistent negative  $T_e$  anomalies) played a dominant role in sustaining cold conditions in 2011. At the same time, the persistent easterly wind anomalies acted to maintain the negative  $T_e$  anomaly pattern. Within the context of the positive thermocline feedback loop, the intensities of the persisting easterly wind anomalies and negative  $T_e$  anomalies were related to each other. Their effects on the second-year cooling in 2011 will be quantified using the ICM-based prediction experiments in the subsequent sections.

## 5 The roles of interannual wind forcing

The wind field is an active element in the thermocline feedback loop, playing an important role in the ENSO evolution. As observed, an easterly wind anomaly persisted over the western-eastern regions during 2010–11, and this anomaly acted to maintain the negative  $T_e$  anomaly pattern. Comparisons with the observations indicated that the ICM can depict the easterly wind anomaly pattern well (but its magnitude was somehow underestimated). In this section, the ICM is used to examine the role played by the easterly wind forcing in the second-year cooling in 2011.

### 5.1 The easterly wind anomaly and its effects

In the SST equation, the SST tendency is affected by various processes, including horizontal advection associated with anomalous currents and vertical mixing/entrainment associated with anomalous  $T_e$  field (Zhang and Gao 2015). Locally, easterly wind anomalies in the western tropical Pacific directly force anomalous currents, which induce a cooling SST tendency through horizontal advection. Additionally, easterly anomalies act to elevate the thermocline, which produces negative  $T_e$  anomalies in the central region, further enhancing a cooling SST tendency in the central and eastern equatorial Pacific.

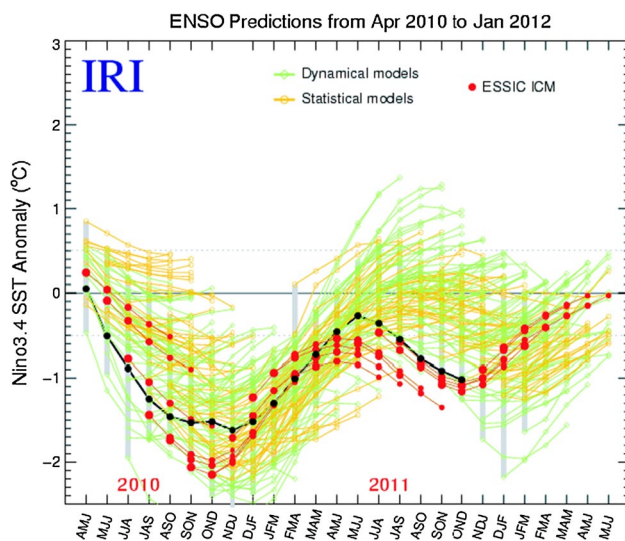


**Fig. 8** The Niño 3.4 SST anomalies (averaged over the region (5°S–5°N; 170°W–120°W)) during 2010–12, observed (*black dotted line*) and predicted (*colored lines*) from different models. Each *colored line* indicates the trajectory of a 5-month forecast made from different initial conditions; results from the ESSIC ICM are *highlighted with the red dotted lines*. Note that this figure is directly taken from the IRI website at: [http://iri.columbia.edu/climate/ENSO/currentinfo/SST\\_table.html](http://iri.columbia.edu/climate/ENSO/currentinfo/SST_table.html)

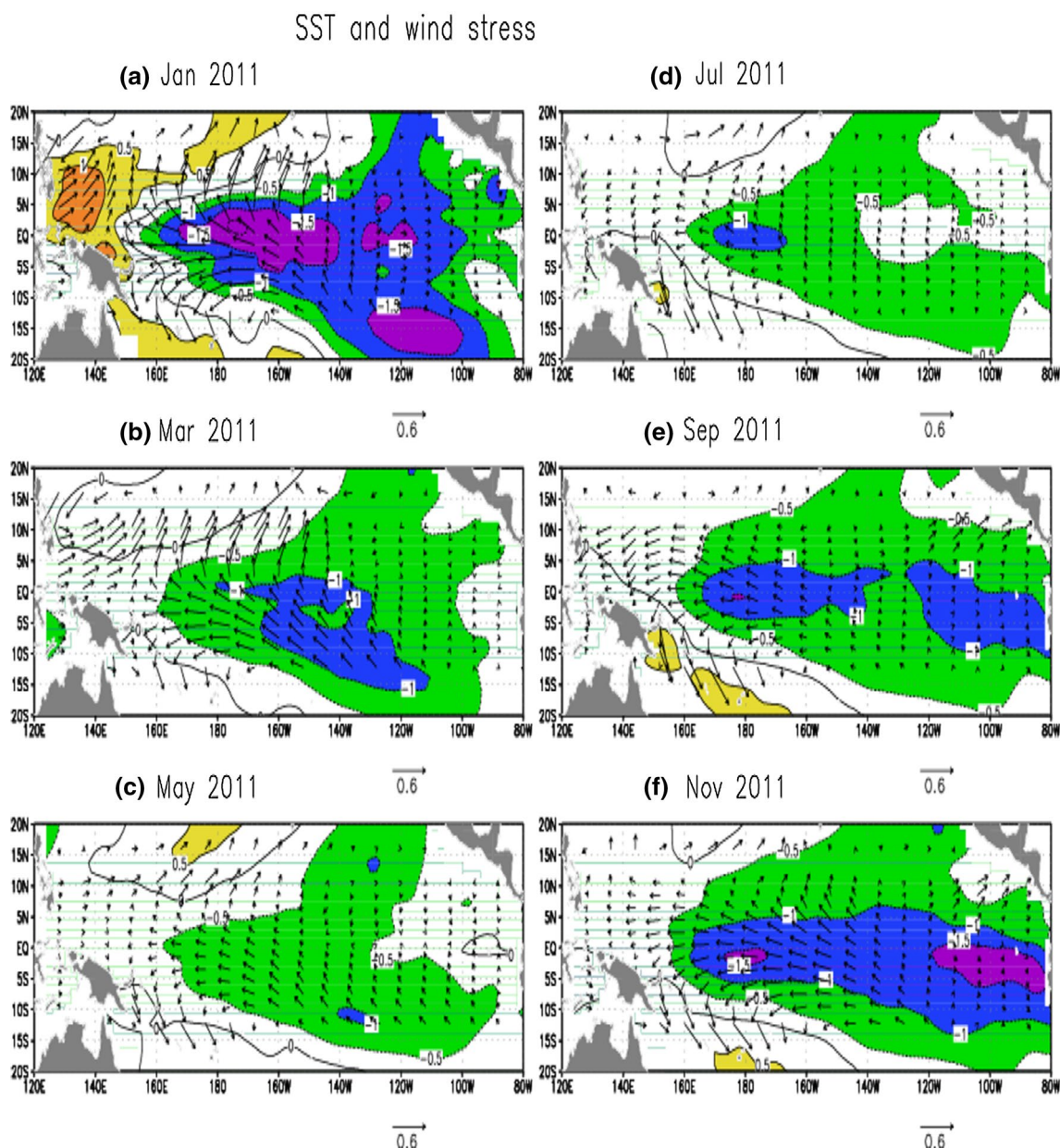


**Fig. 9** Horizontal distributions of monthly mean SST anomalies with the overlaid wind stress anomalies (*vectors*), predicted using the ICM with  $\alpha_\tau = 1.0$  and  $\alpha_{T_e} = 1.0$ , which is initialized from 1 January 2011

for **a** Jan. 2011, **b** Mar. 2011, **c** May 2011, **d** Jul. 2011, **e** Sep. 2011 and **f** Nov. 2011. The contour interval is 0.5 °C for SST, and is dyn cm<sup>-2</sup> for wind stress

The persistence of the easterly wind anomaly and related effects (e.g., in sustaining negative  $T_e$  anomalies) favored the production of a cooling SST tendency over the central-eastern equatorial Pacific in 2011. At the same time, a warming effect from the western Pacific tended to produce a warming SST tendency. Indeed, during May–July 2011, the SST in the eastern equatorial Pacific became slightly warm, but the easterly wind anomaly, though weakened, still persisted in the west-central basin, accompanied by large negative  $T_e$  anomalies there.

The appearance of cold SST anomalies in the east in mid 2011 indicated an important role played by the easterly wind anomalies in concert with the large negative  $T_e$  anomalies.

Thus, the SST evolution into a cooling condition in 2011 can be sensitive to the magnitude of the easterly wind anomalies. It can be envisioned that the easterly wind forcing in the ICM needs to have sufficient intensity to maintain the large negative  $T_e$  anomalies in the equatorial Pacific and thus sustain a cooling SST tendency. It followed that if the

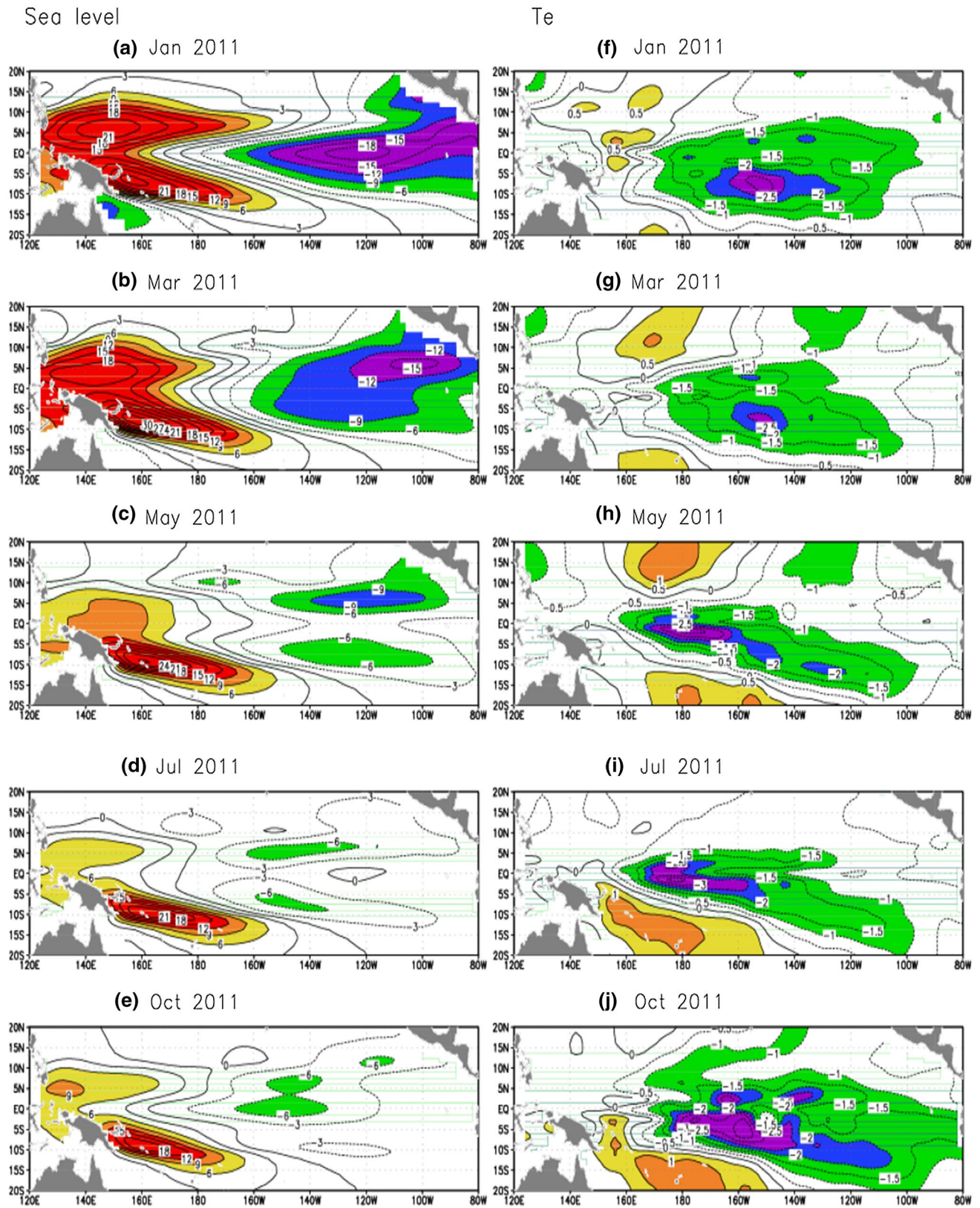


**Fig. 10** The same as in Fig. 6 but for SL and  $T_e$  anomalies predicted using the ICM

Anomalies along the equator

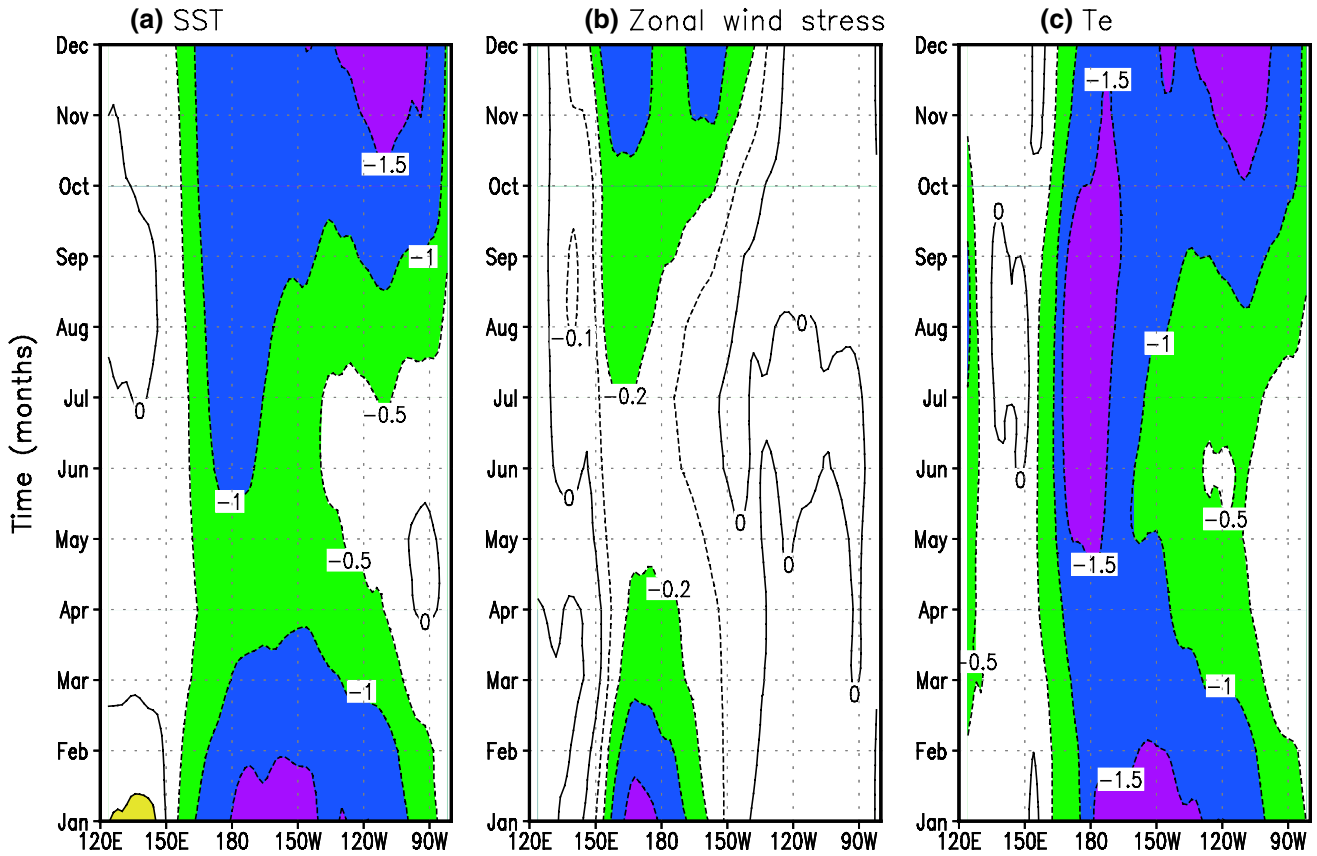
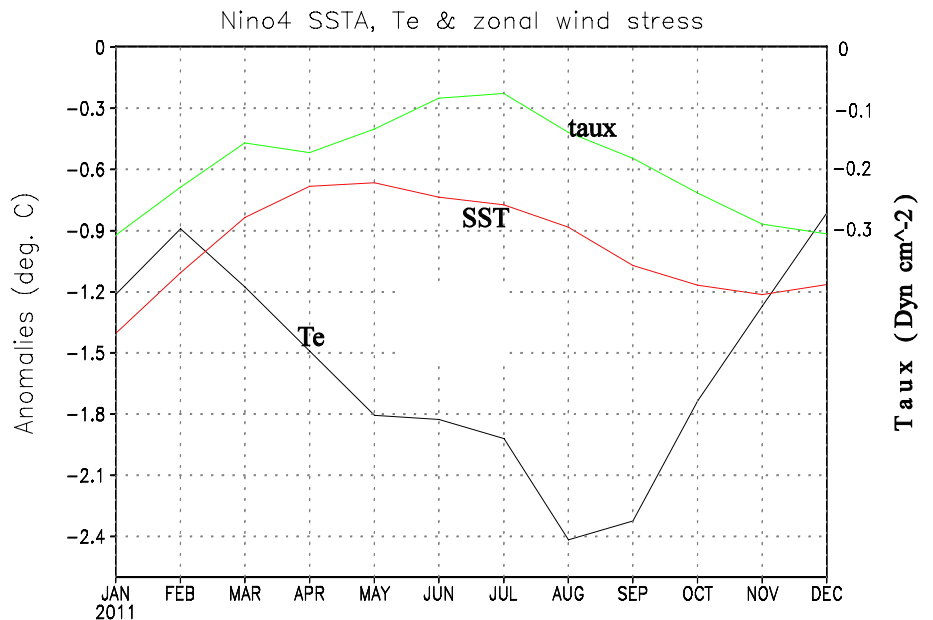


**Fig. 11** Zonal-time sections of anomaly fields along the equator for **a** SST, **b** zonal wind stress and **c**  $T_e$ , which are predicted using the ICM initialized from 1 January 2011. The contour interval is  $0.5\text{ }^\circ\text{C}$  for SST and  $T_e$  and is  $0.1\text{ dyn cm}^{-2}$  for zonal wind stress

**Fig. 12** Time series of anomalies for SST ( $^\circ\text{C}$ ), zonal wind stress ( $\text{dyn cm}^{-2}$  on the *right axis*) and  $T_e$  at the Niño4 site (averaged over the region  $5^\circ\text{S}$ – $5^\circ\text{N}$ ;  $160^\circ\text{E}$ – $150^\circ\text{W}$ ):  $^\circ\text{C}$  on the *left axis*) for year 2011, which are predicted using the ICM from initial conditions on 1 January 2011



amplitudes of the easterly wind anomaly and the negative  $T_e$  anomalies were not adequately represented in a coupled model, the predicted SST tendency could be in a wrong direction (e.g., instead becoming a warming in the fall of 2011 as seen in many coupled model forecasts in Fig. 8). For example, if the easterly wind forcing was underestimated, so might be its effects on the ocean temperature; the resultant weakened negative  $T_e$  anomalies likely led to the weakness or nonexistence of the second-year cooling in 2011. These arguments are tested as described below by prediction experiments using the ICM, in which the easterly wind forcing intensity can be tuned by  $\alpha_\tau$ .

## 5.2 Sensitivity experiments

The intensity of the sustained easterly wind anomaly in the ICM is controlled by the introduced parameter,  $\alpha_\tau$ ; its effects on SST evolution and prediction in 2011 can be examined by varying  $\alpha_\tau$  values. Figures 9 and 10 present examples for the horizontal distributions of some anomaly fields predicted using the ICM with  $\alpha_\tau = 1.0$  and  $\alpha_{T_e} = 1.0$ , which is initialized from 1 January 2011. Figure 13 illustrates the sensitivity of SST predictions to  $\alpha_\tau$ , which again shows that the predictions of the second-year cooling event in 2011 is strikingly successful using the ICM, even made from initial conditions in early 2011. As seen, the changes in  $\alpha_\tau$  have direct effects on the phase transition and the amplitude of the SST anomalies predicted. The larger the  $\alpha_\tau$ , the stronger the wind forcing represented, and the larger the amplitude of the predicted SST anomalies. In particular, when the easterly wind intensity is increased to a certain level, a second-year cooling emerges, which is sustained for a longer

period and is stronger in mid-late 2011. Additionally, an increase in  $\alpha_\tau$  is seen to have a modulating effect on the phase shift from warm conditions to cold conditions as well. In contrast, when  $\alpha_\tau$  is reduced, the wind forcing intensity is weakly represented; the resultant easterly wind response becomes weak over the western-central equatorial Pacific, leading to effects on the ocean that are also weak. In particular, if the wind forcing intensity is represented weakly below certain levels (say  $\alpha_\tau < 0.5$ ), the second-year cooling cannot occur in 2011; instead, a surface warming emerges, with weak SST variability. Thus, adequately depicting the second-year cooling in the ICM requires that the easterly wind forcing intensity be adequately represented up to a certain level. These modeling experiments indicate that the persistent easterly wind forcing is an important factor affecting the second-year cooling in 2011.

## 6 The thermocline effect and its equivalent roles with wind forcing

Another important element in the positive thermocline feedback loop is the role played by the thermal forcing associated with  $T_e$  during ENSO evolution. Previously, the role played by the thermocline effect (as explicitly represented by the relationship between interannual anomalies of SL and  $T_e$ ) in the second-year cooling was demonstrated (Zhang et al. 2013). In this section, sensitivity experiments are conducted to compare the relative effects of subsurface thermal and wind forcings on predictions of the SST evolution during 2010–11.

### 6.1 The thermocline effect and related sensitivity experiments

Previous observations indicated a close relationship between subsurface water entrainment into the mixed layer ( $T_e$ ) and upper-ocean thermal conditions, with the variation of upper-ocean heat content leading Niño3.4 SST anomalies by 1–3 seasons (e.g., Meinen and McPhaden 2000; Hu et al. 2014). In the ICM,  $T_e$  is statistically related to SL, with the lead-lag relation being realized in the  $T_e$  parameterization based on historical data. As we trace the SST evolution in the ICM prediction,  $T_e$  is critically important to the second-year cooling in 2011 (Zhang et al. 2013). In particular, large negative  $T_e$  anomalies persisted in the central equatorial domain, which acted to sustain the cold SST anomaly in the east during July–August 2011. As examined above, there was a warming effect on the SST resulting from the eastward propagation of the positive heat content along the equator, which was accumulated in the western region during 2010. Furthermore, the eastward propagation of positive heat content anomalies along the equator

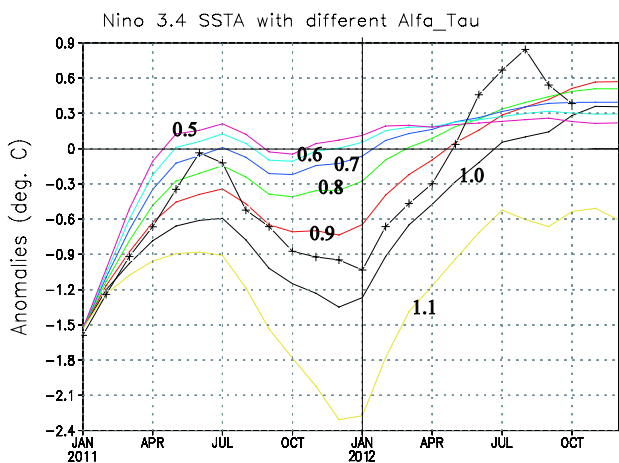


**Fig. 13** The Niño 3.4 SST anomalies during the years 2011–12, observed (the *black line with plus symbol*) and predicted using the ICM from initial conditions on 1 January 2011. Each *line* indicates the predicted trajectory of a 24-month forecast made with  $\alpha_{T_e} = 1.0$  and different values of  $\alpha_\tau$  ranging from  $\alpha_\tau = 0.5$  to  $\alpha_\tau = 1.1$ , respectively

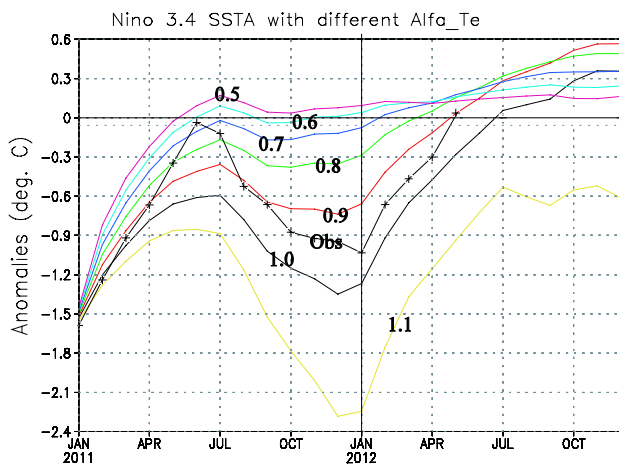


**Fig. 14** The Niño 3.4 SST anomalies during the years 2011–12, observed (the *black line* with *plus symbol*) and predicted using the ICM from initial conditions on 1 January 2011. Each *line* indicates the predicted trajectory of a 24-month forecast made with  $\alpha_\tau = 1.0$  and different values of  $\alpha_{T_e}$  ranging from  $\alpha_{T_e} = 0.5$  to  $\alpha_{T_e} = 1.1$ , respectively

can be inhibited by the persistent negative  $T_e$  anomalies in the central region during 2010–11 (Fig. 7). Thus, the fate of SST variability in the eastern equatorial Pacific in mid 2011 appeared to be determined by these processes in a competing way. As demonstrated by Zhang et al. (2013), the intensity of the negative  $T_e$  anomalies persisted in the central basin is an important factor affecting the second-year cooling in 2011. If its magnitude is reduced somehow, its cooling effect on SST can be weakened and the second-year cooling could not occur in 2011.

Figure 14 exhibits the sensitivity of the Niño 3.4 SST anomalies predicted using the ICM to the intensity of the thermocline effect as represented by varying values of  $\alpha_{T_e}$ . It is seen that reducing the intensity of the negative  $T_e$  anomalies in response to thermocline fluctuation (as indicated in SL) acts to damp the development of cold SST anomalies in 2011. In particular, the cooling in 2011 would not occur if the thermocline effect intensity is weakly represented below certain levels. In such a case, the warming effect associated with the eastward propagation of the positive heat content along the equator could dominate over the reduced cooling effect associated with the negative  $T_e$  anomalies. When the warming effect is strong enough to overcome the cooling effect locally associated with the negative  $T_e$  anomalies, the cold SST condition in the east could be reversed and a warm SST condition could occur in 2011. In contrast, if the negative  $T_e$  anomalies can maintain its intensity to a certain level, the cooling effect can overwhelm the warming effect. The fact that the SST became cooling in 2011 indicated that the persistent negative  $T_e$  anomalies in the central- eastern Pacific exerted a dominant

influence relative to the warming effect from the western tropical Pacific. As the cold SST anomalies emerged in the east, the easterly wind anomalies can be reasonably considered as a corresponding response. These SST and wind anomalies formed coupled interactions within the tropical Pacific, leading to the double-dip evolution of SST in 2011.

## 6.2 The equivalent roles of the $T_e$ and wind forcing effects

The above analyses indicate that the sustained negative  $T_e$  anomaly pattern and easterly wind forcing both play an important role in the SST cooling in 2011. In fact, they are related to each other as these two elements participate in the same thermocline feedback loop. As a result, the magnitude of the negative  $T_e$  anomalies is directly related to the intensity of the easterly wind forcing, with the latter acting to sustain the former. Thus, the roles played by wind and  $T_e$  fields can be equivalent in terms of their effects on the SST prediction. These arguments can be tested using ICM-based experiments.

By comparing Figs. 13 and 14, it is evident that the effect on the SST prediction induced by changing the intensity of wind forcing (tuning  $\alpha_\tau$ ) is equivalent to that induced by changing the intensity of the  $T_e$  anomalies (tuning  $\alpha_{T_e}$ ). The predicted SST evolution is more or less the same because the effect due to a decreased intensity of one forcing tends to be compensated by an increased intensity of the other. These prediction experiments indicate that the intensity of the negative  $T_e$  anomalies and easterly wind anomalies can be equally important to the second-year cooling. Figures 15 and 16 further illustrate the horizontal distributions of monthly mean SST and wind stress anomalies, predicted using the ICM with  $\alpha_\tau = 1.2/\alpha_{T_e} = 0.8$  and  $\alpha_\tau = 0.8/\alpha_{T_e} = 1.2$ , respectively. The predicted structure and amplitude of cold SST anomalies in the two experiments are very similar to each other. Taking Figs. 13 and 14 together, it is clearly demonstrated that the thermocline effect (as represented by the relationship between  $T_e$  and SL) and wind forcing play an equivalent role in the second-year cooling during the 2010–12 La Niña event.

These results can be useful to explain why a coupled model may fail to predict the second-year cooling in 2011. As analyzed above, various processes are involved and compete in their effects on the SST evolution in the eastern equatorial Pacific in 2011 (Fig. 7), mainly including the warming effect resulting from the eastward propagation of the positive heat content along the equator, and the cooling effect locally associated with persistent negative  $T_e$  anomalies which are associated with the easterly wind anomalies. As the fate of SST is determined by the subtle balance among the effects of these processes, they need to be represented adequately in coupled models. As illustrated using



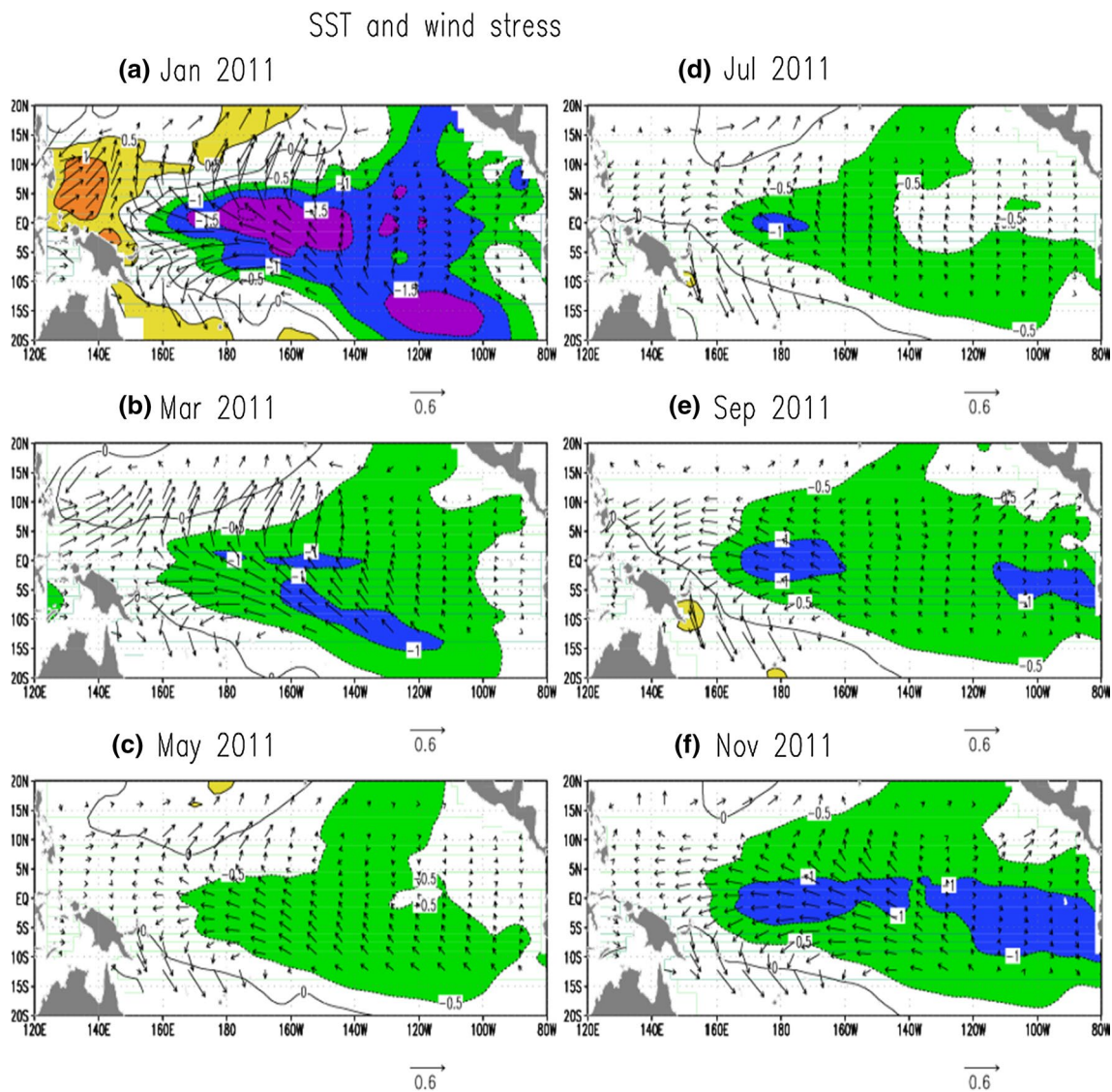


**Fig. 15** The same as in Fig. 9 but predicted using the ICM with  $\alpha_\tau = 1.2$  and  $\alpha_{T_e} = 0.8$

the ICM, the effects of wind and thermal fields on the SST prediction are sensitive to the ways in which they are represented. Since the SSTs in the eastern equatorial Pacific became cooling in August 2011, the warming effect was not sufficiently strong to reverse the cold condition that was associated with the negative  $T_e$  anomalies. It follows that if the amplitude of the easterly wind anomalies and negative  $T_e$  anomalies were underestimated, the predicted SST tendency can be in a wrong direction.

## 7 Conclusion and discussion

Observations showed the “double dip” evolution of SST in 2011 that followed the La Niña event in 2010. Great challenges exist in making accurate real-time SST predictions

for the year 2011 from initial conditions in early and middle 2011 because so many coupled ocean–atmosphere models fail to capture the second-year cooling in 2011. There is an urgent need to understand the processes leading to the cooling and to improve real-time ENSO forecasts.

Persistent anomaly conditions in the tropical Pacific involve the positive thermocline feedback through interactions among the SST, surface winds and thermocline. During 2010–12, the tropical Pacific experienced a prolonged cold condition. Following the La Niña event that peaked in Oct. 2010, several factors affected the SST condition in the eastern equatorial Pacific in 2011. For example, a warming effect was associated with the eastward propagation of the positive heat content anomalies from the west to east on the equator in early 2011. Its arrival to the east in mid 2011 tended to produce a warming effect on SST. Indeed, a

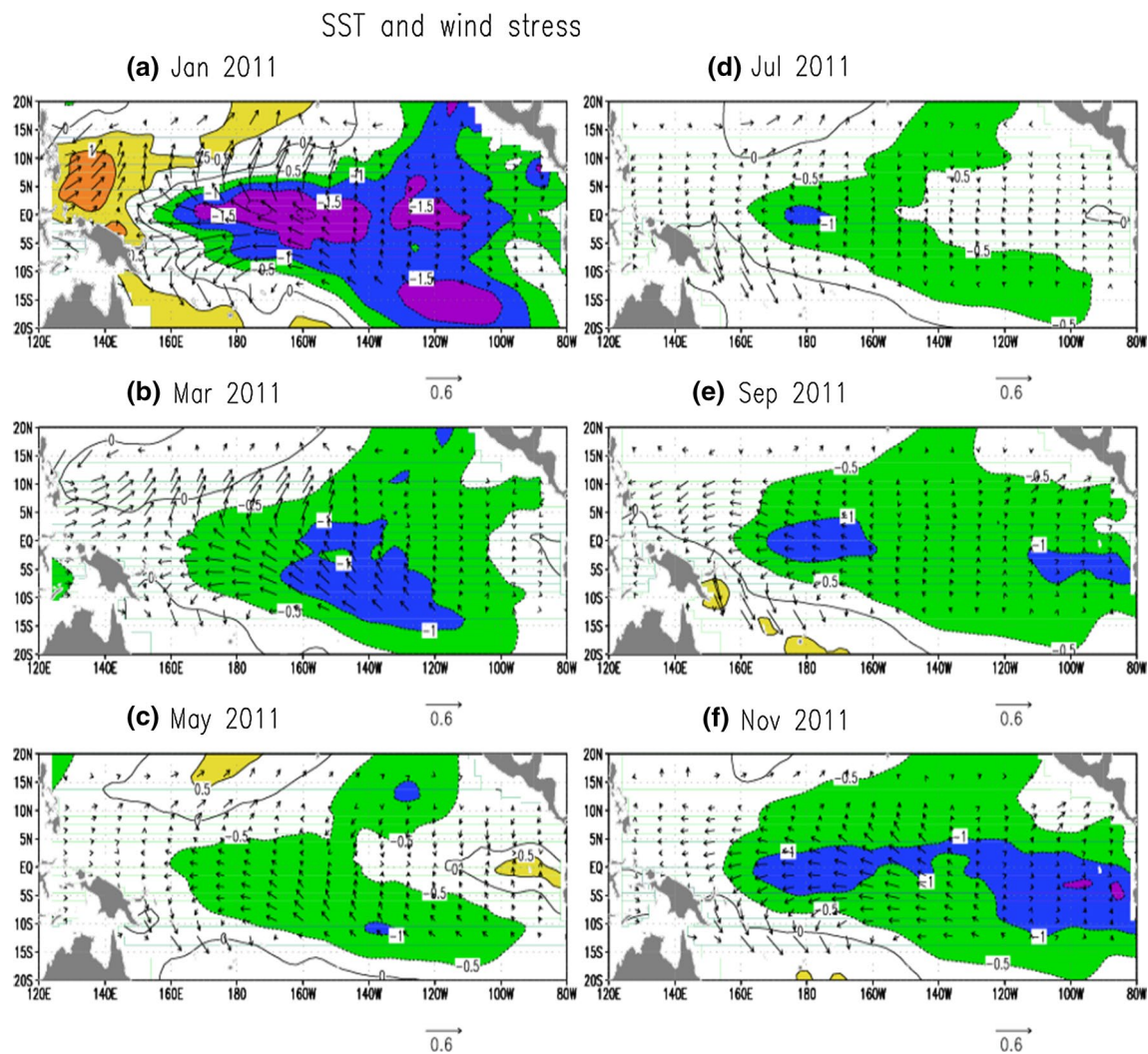


**Fig. 16** The same as in Fig. 15 but predicted using the ICM with  $\alpha_\tau = 0.8$  and  $\alpha_{T_e} = 1.2$

nearly normal SST condition emerged in the eastern equatorial Pacific in mid 2011. However, there existed a cooling effect that was associated with negative  $T_e$  anomalies in the central-eastern equatorial Pacific, characterized by the horseshoe-like  $T_e$  pattern. Additionally, persistent easterly wind anomaly in the central-eastern equatorial Pacific was in favor of a SST cooling in the east. As such, these competing processes collectively determined the SST condition in the eastern equatorial Pacific, with their net effects (either cooling or warming), depending on which was more dominant over the other. The fact that SSTs became cool in 2011 suggested the dominant role played by the persistent negative  $T_e$  anomalies and easterly wind anomalies in the equatorial Pacific. Several factors were responsible for the persistent negative  $T_e$  anomaly pattern as displayed in Fig. 7. For example, one striking feature on the atmospheric side was the persistence of easterly wind anomalies in the western-central equatorial Pacific, making a contribution

to sustaining negative  $T_e$  anomalies in the central-eastern equatorial Pacific. As the thermocline effect and wind forcing participated in the same feedback loop, they can play a similar role in determining the SST evolution. These qualitative arguments are tested by ICM-based numerical experiments in the prediction context of the second-year cooling in 2011. In our previous modeling study, we demonstrated that the ICM can predict the correct SST evolution during 2010–12, including the two transitional points, one in June 2011 from warming to cooling, and another in January 2012 from cooling to warming. Furthermore, the ICM is used to demonstrate a critically important role played by subsurface  $T_e$  effects in the second-year cooling in 2011.

In this paper, we illustrate the roles played by atmospheric wind forcing in the second-year cooling in 2011. In the ICM we use, the atmospheric model was a simple statistical one relating interannual wind variability to SST anomalies. One observed feature during 2010–11 is the

sustained easterly wind anomalies over the central equatorial Pacific. The easterly wind anomaly, which persisted over the western-central Pacific during 2010–11, acted to sustain the horseshoe-like  $T_e$  pattern connecting large negative subsurface thermal anomalies off and on the equator. Additionally, the easterly wind anomalies induced current anomalies locally. As the easterly wind anomalies participated to maintain the cold anomaly of entrained waters into the mixed layer, wind forcing can play a role in the development of the cold SST anomalies in 2011. Sensitivity experiments are conducted to demonstrate the extent to which the second-year cooling forecasts were affected by the intensity of the easterly wind anomaly. The strength of the easterly wind anomaly in the western-central Pacific is shown to be important for the correct prediction of the cold SST anomalies in 2011. Furthermore, as two elements of the positive thermocline feedback loop, wind forcing and thermocline effect are both important. Prediction experiments are compared to quantify the relative roles of the two elements in the realistic prediction of the second-year cooling in the fall of 2011. It is illustrated that the  $T_e$  effect and the easterly wind forcing is equally important to the SST evolution during 2010–11.

This modeling study presents a clear picture of how the second-year cooling can emerge in the tropical Pacific climate system. Following 2010, a positive heat content anomaly exhibited eastward propagation along the equator from the western Pacific region; its arrival to the east acted to produce a warming effect on SST. Locally, negative  $T_e$  anomalies prevailed in the central-eastern equatorial Pacific, acting to sustain cold SST conditions in the east. The fact that SSTs in the east became cooling in the tropical Pacific in August 2011 indicated that the warming effect from the west was not sufficiently strong to overcome the cooling effect locally associated with the negative  $T_e$  anomalies and easterly wind anomalies. The net effect was a cooling in the eastern equatorial Pacific. Thus, capturing the cooling in 2011 requires a balanced representation of warming effect remotely from the western Pacific and the cooling effect locally associated with the negative  $T_e$  anomalies and easterly wind anomalies in the central equatorial Pacific. Using the ICM, it is demonstrated that the intensities of the wind forcing and thermocline effect need to be represented up to a certain level to predict the second-year SST cooling in mid-late 2011. These results provide an improved predictive understanding for the equivalent roles played by wind and  $T_e$  forcings in the SST prediction.

These analyses clearly suggest that the evolution into the second-year cooling from year 2010–2011 is different from what is inferred from the current theories of ENSO. For example, the so-called delayed oscillator paradigm has been proposed to explain ENSO cycles within the tropical Pacific climate system, serving as a negative feedback

for ENSO. The phase reversal in this scenario is realized by a downwelling equatorial Rossby wave that is generated midbasin at the peak of La Niña events and propagates westward off the equator towards the western boundary, then reflects and returns on the equator as an eastward-propagating equatorial Kelvin wave. Its arrival to the east acts to reverse the cold phase. We can apply this ENSO theory to the second-year cooling in 2011. Following the La Niña event in 2010, there was a signal propagating along the equator from the western Pacific towards the east, representing a warming effect on SST in the east. Its arrival to the east would reverse the cold SST condition and produce a warm condition as expected from the delayed oscillator theory. Indeed, a nearly normal SST condition emerged in mid 2011 for a short while. The cold condition then continued in summer 2011 and intensified in fall of 2011. At this time, there is no cooling signal propagating from the western boundary (and thus the cooling in the east cannot be explained from this). So, local processes must play a role in the cooling in the eastern-central equatorial Pacific. One emphasis from this study is the role played by the negative  $T_e$  anomaly pattern in the equatorial Pacific. As analyzed and tested using the ICM, the cooling is attributed to the persistence of large negative  $T_e$  anomalies in the eastern-central equatorial Pacific. Furthermore, it is evident that several processes contribute to sustaining the negative  $T_e$  anomalies, including off-equatorial influences and the persisted easterly wind anomalies in the equatorial Pacific (Fig. 7).

This is only a case study based on a simplified model with obvious limitations. The results can be model and/or case dependent. Further prediction experiments are underway to extend this case study. For example, it is planned to make predictions for other historical cases with La Niña events having second-year cooling to better characterize the SST evolution as observed in 2011 (e.g., Hu et al. 2014). Additionally, specific questions need to be addressed. For instance, can the processes analyzed for the 2011 case also be applicable to other historical periods with a second-year cooling? Given the skill of this ICM relative to other coupled models, what are the specific “missing mechanisms” characteristic of others that fail to predict the second-year cooling? Are the mechanisms identified from this ICM also working in other coupled models? In addition, the ICM tends to have a cold bias in its SST simulations (e.g., Zhang et al. 2005b). Does this affect the sensitivity results presented in this paper and in Zhang et al. (2013)? More analyses and modeling experiments will be presented elsewhere.

**Acknowledgments** We would like to thank A. J. Busalacchi, Jiayu Zhou, A. G. Barnston, Z.-Z. Hu, C. Wang and J. Lu for their comments. The author wishes to thank the two anonymous reviewers for their numerous comments that helped to improve the original manuscript. We benefited greatly from the CPC’s ocean briefing

for providing real-time diagnostic and prediction discussions for the evolution of the 2010–11 La Niña event; see the summary on the STIP web page made by Jiayu Zhou. This research is supported by the National Natural Science Foundation of China (Grant Nos. 41490644, 41475101 and 41421005), the CAS Strategic Priority Project (the Western Pacific Ocean System (WPOS; Project Nos. XDA11010105, XDA11020306 and XDA11010301), the NSFC-Shandong Joint Fund for Marine Science Research Centers (Grant No. U1406401), and the NSFC Innovative Group Grant (Project No. 41421005).

**Open Access** This article is distributed under the terms of the Creative Commons Attribution 4.0 International License (<http://creativecommons.org/licenses/by/4.0/>), which permits unrestricted use, distribution, and reproduction in any medium, provided you give appropriate credit to the original author(s) and the source, provide a link to the Creative Commons license, and indicate if changes were made.

## References

- Barnett TP, Latif M, Graham N, Flugel M, Pazan S, White W (1993) ENSO and ENSO-related predictability. Part I: prediction of equatorial Pacific sea surface temperature with a hybrid coupled ocean–atmosphere model. *J Clim* 6:1545–1566
- Barnston AG, Tippett MK, L'Heureux ML, Li S, DeWitt DG (2012) Skill of real-time seasonal ENSO model predictions during 2002–11: is our capability increasing? *Bull Am Meteorol Soc* 93:631–651
- Battisti DS, Hirst AC (1989) Interannual variability in the tropical atmosphere–ocean system: influences of the basic state, ocean geometry and nonlinearity. *J Atmos Sci* 46:1687–1712
- Bjerknes J (1969) Atmospheric teleconnections from the equatorial Pacific. *Mon Weather Rev* 97:163–172
- Cane MA, Zebiak SE, Dolan SC (1986) Experimental forecast of El Niño. *Nature* 321:827–832
- Chen D, Zebiak SE, Busalacchi AJ, Cane MA (1995) An improved procedure for El Niño forecasting: implications for predictability. *Science* 269:1699–1702
- DiNezio PN, Deser C (2014) Nonlinear controls on the persistence of La Niña. *J Clim* 27:7335–7355. doi:10.1175/JCLI-D-14-00033.1
- Feng L, Zhang RH, Wang Z, Chen X (2015) Processes leading to the second-year cooling of the 2010–12 La Niña event, diagnosed from GODAS. *Adv Atmos Sci* 32:424–438. doi:10.1007/s00376-014-4012-8
- Gu D, Philander SGH (1997) Interdecadal climate fluctuations that depend on exchanges between the tropics and extratropics. *Science* 275(5301):805–807
- Hu ZZ, Kumar A, Xue Y et al (2014) Why were some La Niñas followed by another La Niña? *Clim Dyn* 42(3):1029–1042
- Ji M, Leetmaa A, Kousky VE (1996) Coupled model forecasts of ENSO during the 1980 and 1990s at the National Meteorological Center. *J Clim* 9:3105–3120
- Jin F-F (1997) An equatorial ocean recharge paradigm for ENSO. Part I: conceptual model. *J Atmos Sci* 54:811–829
- Jin F-F, An S (1999) Thermocline and zonal advective feedbacks within the equatorial ocean recharge oscillator model for ENSO. *Geophys Res Lett* 26(19):2989–2992. doi:10.1029/1999GL002297
- Kalnay E et al (1996) The NMC/NCAR reanalysis project. *Bull Am Meteorol Soc* 77:437–471
- Keenlyside N, Kleeman R (2002) On the annual cycle of the zonal currents in the equatorial Pacific. *J Geophys Res*. doi:10.1029/2000JC000711
- Kirtman B, Fan Y, Schneider EK (2002) The COLA global coupled and anomaly coupled ocean–atmosphere GCM. *J Clim* 15:2301–2320
- Latif M et al (1998) A review of the predictability and prediction of ENSO. *J Geophys Res* 103:14375–14393
- Lee S-K, DiNezio PN, Chung E-S, Yeh S-W, Wittenberg AT, Wang C (2014) Spring persistence, transition, and resurgence of El Niño. *Geophys Res Lett* 41:8578–8585. doi:10.1002/2014GL062484
- Luo JJ, Masson S, Behera S, Shingu S, Yamagata T (2005) Seasonal climate predictability in a coupled OAGCM using a different approach for ensemble forecasts. *J Clim* 18:4474–4497
- McCreary JP (1981) A linear stratified ocean model of the equatorial undercurrent. *Philos Trans R Soc (Lond)* 298:603–635
- McPhaden MJ, Zebiak SE, Glantz MH (2006) ENSO as an integrating concept in Earth Science. *Science* 314:1740–1745
- Meinen CS, McPhaden MJ (2000) Observations of warm water volume changes in the equatorial Pacific and their relationship to El Niño and La Niña. *J Clim* 13:3551–3559
- Okumura M, Deser C (2010) Asymmetry in the duration of El Niño and La Niña. *J Clim* 23:5826–5843. doi:10.1175/2010JCLI3592.1
- Picaut J, Masia F, du Penhoat Y (1997) An advective-reflective conceptual model for the oscillatory nature of the ENSO. *Science* 227:663–666
- Reynolds RW, Smith TM (1994) Improved global sea surface temperature analyses using optimum interpolation. *J Clim* 7(6):929–948
- Reynolds RW, Rayner NA, Smith TM, Stokes DC, Wang W (2002) An improved in situ and satellite SST analysis for climate. *J Clim* 15:1609–1625
- Saha S et al (2006) The NCEP climate forecast system. *J Clim* 19:3483–3517
- Schopf and Suarez (1988) Vacillations in a coupled ocean–atmosphere model. *J Atmos Sci* 45:549–566
- Stockdale TN et al (2011) ECMWF seasonal forecast system 3 and its prediction of sea surface temperature. *Clim Dyn* 37:455–471. doi:10.1007/s00382-010-0947-3
- Wang C (2001) A unified oscillator model for the El Niño–southern oscillation. *J Clim* 14:98–115
- Wang C, Picaut J (2004) Understanding ENSO physics—a review. In: Wang C, Xie S-P, Carton JA (eds) *Earth's climate: the ocean–atmosphere interaction*, vol 147. AGU Geophysical Monograph Series, Washington, DC, pp 21–48
- Wang C, Weisberg RH, Virmani JI (1999) Western Pacific interannual variability associated with El Niño–southern oscillation. *J Geophys Res* 104(C3):5131–5149
- Wang W, Chen M, Kumar A (2010) An assessment of the CFS real-time seasonal forecasts. *Weather Forecast* 25:950–969
- Weisberg RH, Wang C (1997) A western Pacific oscillator paradigm for the El Niño–southern oscillation. *Geophys Res Lett* 24:779–782
- Zebiak SE, Cane MA (1987) A model El Niño/southern oscillation. *Mon Weather Rev* 115:2262–2278
- Zhang R-H, Zebiak SE, Kleeman R et al (2003) A new intermediate coupled model for El Niño simulation and prediction. *Geophys Res Lett* 30(19):2012. doi:10.1029/2003GL018010
- Zhang R-H, Kleeman R, Zebiak SE, Keenlyside N, Raynaud S (2005a) An empirical parameterization of subsurface entrainment temperature for improved SST simulations in an intermediate ocean model. *J Clim* 18:350–371

- Zhang R-H, Zebiak SE, Kleeman R, Keenlyside N (2005b) Retrospective El Niño forecast using an improved intermediate coupled model. *Mon Weather Rev* 133:2777–2802
- Zhang R-H, Busalacchi AJ, DeWitt DG (2008) The roles of atmospheric stochastic forcing (SF) and oceanic entrainment temperature ( $T_e$ ) in decadal modulation of ENSO. *J Clim* 21:674–704
- Zhang R-H, Zheng F, Zhu J, Wang ZG (2013) A successful real-time forecast of the 2010–11 La Niña event. *Sci Rep* 3:1108. doi:[10.1038/srep01108](https://doi.org/10.1038/srep01108)
- Zhang R-H, Gao C (2015) Role of subsurface entrainment temperature ( $T_e$ ) in the onset of El Niño events, as revealed in an intermediate coupled model. *Clim Dyn*. doi:[10.1007/s00382-015-2655-5](https://doi.org/10.1007/s00382-015-2655-5)
- Zhang R-H, Gao C, Kang X, Zhi H, Wang Z, Feng L (2015) ENSO modulations due to interannual variability of freshwater forcing and ocean biology-induced heating in the tropical Pacific. *Sci Rep* 5:18506. doi:[10.1038/srep18506](https://doi.org/10.1038/srep18506)
- Zheng F, Zhu J, Zhang R-H, Zhou G-Q (2006) Ensemble hindcasts of SST anomalies in the tropical Pacific using an intermediate coupled model. *Geophys Res Lett* 33:L19604. doi:[10.1029/2006GL026994](https://doi.org/10.1029/2006GL026994)
- Zhu J, Huang B, Marx L, Kinter JL III, Balmaseda MA, Zhang R-H, Hu ZZ (2012) Ensemble ENSO hindcasts initialized from multiple ocean analyses. *Geophys Res Lett* 39(9). doi:[10.1029/2012GL051503](https://doi.org/10.1029/2012GL051503)
- Zhu J, Huang B, Zhang R-H et al (2014) Salinity anomaly as a trigger for ENSO events. *Sci Rep* 4:6821. doi:[10.1038/srep06821](https://doi.org/10.1038/srep06821)